6-1996

Residual Strength after Fatigue of Unidirectional and Cross-Ply Metal Matrix Composites at Elevated Temperature

Sen-Tzer Chiou

AD-A286 886

RESIDUAL STRENGTH AFTER FATIGUE
OF UNIDIRECTIONAL AND CROSS-PLY
METAL MATRIX COMPOSITES
AT ELEVATED TEMPERATURE

THESIS

Sen-Tzer Chiou, Major, R. O. C., ARMY

AFIT / GAE / ENY / 96 1 2

96-01650

DEPARTMENT OF THE AIR FORCE

AIR UNIVERSITY

AIR FORCE INSTITUTE OF TECHNOLOGY

Wright-Patterson Air Force Base, Ohio

RESIDUAL STRENGTH AFTER FATIGUE
OF UNIDIRECTIONAL AND CROSS-PLY
METAL MATRIX COMPOSITES
AT ELEVATED TEMPERATURE

THESIS

Sen-Tzer Chiou, Major, R. O. C., ARMY

AFIT / GAE / ENY / 96 J-2

DISCLAIMER NOTICE

THIS DOCUMENT IS BEST
QUALITY AVAILABLE. THE COPY
FURNISHED TO DTIC CONTAINED
A SIGNIFICANT NUMBER OF
COLOR PAGES WHICH DO NOT
REPRODUCE LEGIBLY ON BLACK
AND WHITE MICROFICHE.

RESIDUAL STRENGTH AFTER FATIGUE OF UNIDIRECTIONAL
AND CROSS-PLY METAL MATRIX COMPOSITES
AT ELEVATED TEMPERATURE

THESIS

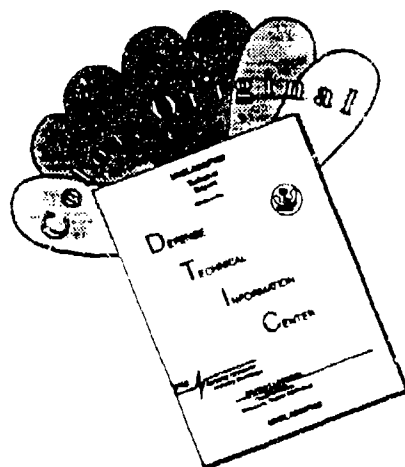Presented to the Faculty of the School of Engineering

of the Air Force Institute of Technology

Air University

in Partial Fulfillment of the

Requirements for the Degree of

Master of Science in Aeronautical Engineering

Sen-Tzer Chiou, Major, R. O. C., ARMY

June, 1996

Acknowledgements

The first thing I want to say my thanks to the Department of Aeronautical and Astronautical Engineering, School of Engineering for providing this topic for me to study the metal matrix composite's behavior under fatigue condition.

There are many persons whom I would like to express my greatest gratitude, such as my thesis advisor, Dr. Robertson, Dr. Mall, Dr. Torvik, Dr. Shaker, Mark Derisso, Christopher Kelley, Sean Coghlan, Dan Rioux, Jay Anderson, J. J. Schubbe, Dr. Li , and my wife, Lindy. Especially, I want to present my deep appreciation to Dr. Robertson for correcting, providing, giving valuable suggestions on this work. If not for their help, instructions, and encourgement, this work couldn't be finished. I was constantly thinking " how to do these tests and what's the main objective? ". I really very much appreciate these people for a great deal of patience and considerations for helping me to accomplish this work.

ii

Table of Contents

iv

List of Figures

vii

List of Tables

Abstract

This study investigated the residual strength of the unidirectional and cross-ply laminates of SCS-6 / Ti-15-3, metal matrix composite at elevated temperature 427°C (800°F) after under tension-tension load controlled mode. For this purpose, several specimens were fatigued to various fractions of the fatigue life and then loaded monotonically to failure. The purpose of this study was to determine the effects of different levels of fatigue damage on the composite's strength.

The unidirectional specimens were cycled at a 900 MPa maximum stress at a frequency of 10 Hz, while, the cross-ply specimens were tested at both 300 MPa and 450 MPa at 5 Hz and 10 Hz, respectively. The residual strength results for the three cases showed similar trends in that residual strength drop with cycles was small until near the end of the fatigue life. Both the unidirectional and cross-ply specimens demonstrated only a small drop of the residual strength with cycles until near the end of the fatigue life. Thus, the material exhibits a critical or catastrophic failure behavior as the presence of damage must reach a critical level before it has much effect on the composite.

The failure mode for the monotonic tests was dominated by the strength of the fibers for both longitudinal and cross-ply laminates. Also, the inelastic deformation of the composite was found to be dominated by matrix plasticity. For the fatigue tests, debonding between fibers and matrix was found, which produced crack initiation sites. These crack initiation sites were observed on both the surface of and internal within the specimens. Matrix cracks from these damage sites proceeded to propagate transverse to the load and fiber directions.

Residual Strength After Fatigue of Unidirectional and Cross-Ply Metal Matrix Composites at Elevated Temperature

1.*Introduction*

Metal matrix composites materials have several advantages compared to metallic materials. They possess higher rigidity and specific strength, good oxidation resistance and considerable flexibility in high temperature applications. In many aerospace and other applications, metal- matrix composites (MMC) will be subjected to fatigue loading along with a superimposed variation in temperature, so structural components must perform well under a wide range of mechanical and thermal loading conditions. MMCs could provide the fatigue endurance to survive high temperature and high stress environments. They are, therefore, currently being developed for high temperature applications in engine and structures of hypersonic flight vehicles which require a stiff, light weight material capable of carrying significant thermal and mechanical loads.

There are three basic matrix categories of composite materials (ceramic matrix, polymeric matrix, and metal matrix composites). Ceramic matrix composites are usually ceramic fibers embedded in a ceramic matrix. They have excellent properties at high temperature because of their thermal characteristics, but are too brittle for most applications. Polymeric composites are generally composed of graphite fibers embedded in a polymer matrix. They have good strength characteristics, but poor thermal properties. Metal matrix composites blend excellent characteristics of maintaining good mechanical properties at high temperature conditions for aerospace applications.

1

Titanium-based metal-matrix composites, such as SCS-6/Ti-15-3 and SCS-6/Ti-6-4, have been studied extensively because the titanium alloy matrix can be used at high temperature, and these composites have higher specific strength than any conventionally structural materials. A titanium-based alloy reinforced with continuous silicon carbide fibers, SCS-6/Ti-15-3, which exhibits a high strength-to-weight ratio (stiffness, strength, fracture toughness) and good thermal resistance, is a good model material to study the basic features of titanium metal-matrix composites. In an uncoated state, the SiC/Ti-15-3, a good model composite system has a potential application temperature ranging from room temperature up to 550°C. The composite must be coated for use above 550°C to prevent excessive oxidation of the matrix [1].

The unidirectional $[0]_8$ and cross-ply $[0/90]_{2s}$ laminates of SCS-6/Ti-15-3 metal-matrix composite are the subject of the present study. Before these materials can be used effectively in aerospace design, they must be fully characterized. A parameter, a very important to designers, is the material's residual strength. This represents its remaining strength after it has undergone some prior load history. The present work seeks to investigate this parameter after fatigue loading.

The primary objective of the present work is to characterize the residual strength of the unidirectional and cross-ply laminates of the SCS-6/Ti-15-3, a titanium alloy matrix based composite. Tension-tension fatigue loading of the laminates were conducted and then stopped at a given number of cycles. These specimens were then monotonically loaded to failure to determine the residual strength. All tests were conducted under an isothermal environment at an elevated temperature of 427°C with a minimum load to

2

maximum load ratio, R, of 0.05. Loading frequencies of 5 Hz and 10 Hz were used with a triangular waveform. Both the fatigue and monotonic tests were conducted under load-control mode, and all monotonic loads to failure were conducted at the rate of 15 MPa/s. Assessing the long-term properties requires analysis of the basic mechanisms of degradation and incorporation of this knowledge in development of appropriate material models. Analyses of composite damage must take an interdisciplinary approach, combining the physics of damage and the mechanics of solids. Therefore, the present study will also examine the microstructural damage mechanisms leading to failure to provide the basis for choosing appropriate models.

2. *Previous Works*

A fatigue phenomenon has three distinct regions. The first is the initiation of the crack which occurs at a location of high stress concentration. For a fiber reinforced metal matrix composite material, crack initiation usually occurs either at the surface or at the interface of the fiber and matrix. The second region is the crack propagation which will vary depending on the composite construction and layup. Metal matrix fiber reinforced composites are of a layered construction. Each layer is composed of either fiber mats or the metal matrix fail. The third region is characterized by rapid crack propagation followed by fracture.

Unidirectional fiber reinforced composites possess excellent fatigue resistance in the fiber direction which carries most of the load. Fatigue damage within a composite occurs in one or more forms such as failure of the fiber and matrix interface, matrix cracking, fiber breaking, and ply delamination. The nature of the fatigue will vary not only between composites of different constituent materials but also between composites of different constructions and layup. Fatigue failures result from repeated loading and unloading of a given structure. At higher load, a given structure will have a much shorter life. Contrary, at the lower load, the life is apparently longer.

Johnson, Lubowinski, and Highsmith conducted fatigue tests of SCS-6/Ti-15-3 [2]. These tests were performed on five different lay-ups, $[0]_8$, $[90]_8$, $[0_2/\pm45]_s$, $[0/90]_{2s}$, and $[0/\pm45/90]_s$ at room temperature and a cyclic frequency of 10 Hz. The stress in the 0° fibers was determined through a micromechanics approach, and a correlation was made to

4

determine the fatigue life of different laminates containing 0° plies. Such correlations may be useful for predicting the fatigue life of various types of layups.

Gabb, Gayda, and Mackay also investigated the fatigue behavior of SCS-6 / Ti-15-3 unidirectional metal-matrix composite, but at elevated temperatures of 300^oC and 550^oC as well as under nonisothermal conditions [3]. They performed fatigue life tests in a load controlled mode (stress basis) and concluded that the matrix didn't control the fatigue life of the composite. At high stress level and at 550^oC, fiber and matrix interface crack initiation followed by matrix crack propagation was thought to limit the fatigue life of the composites. They found that the composite showed an increase in mean strain, due to the creep of the matrix, over the fatigue life test at 550^oC. However, at 300^oC, the mean strain remained constant throughout the fatigue life test. They also observed that although the fatigue life of the composite exceed that of the matrix alloy on a stress basis, the fatigue life of the matrix exceeded that of the composite on a strain basis.

Castelli, Ellis, and Bartolotta investigated the thermomechanical (from 93^oC to 540^oC) and isothermal (427^oC) fatigue behavior of the SCS-6/Ti-15-3 metal matrix composite [4]. They found that the fatigue lives were significantly reduced under thermomechanical conditions when compared to those obtained under the comparable isothermal conditions. They also observed that cyclic mean strain significantly increased over the first several thousand cycles and continued to increase gradually throughout the life of the specimens. This suggests that creep cannot be ignored at this temperature of 427^oC.

Lerch and Saltsman made an investigation into the damage mechanisms produced by tensile loads at room temperature (RT) and 427°C for various layup's of the SCS-6/Ti-15-3 composite system ($[0]_8$, $[90]_8$, $[\pm30]_s$, $[0/90]_{2s}$, $[0/\pm45/90]_s$) [5]. The damage was examined through microscopic evaluation, and a micromechanical stress analysis program (ANGPLY) was used to understand the observed damage mechanisms.

An additional study of the unidirectional SCS-6/Ti-15-3 fatigue behavior at high temperature (650°C) was conducted by Pollock and Johnson [6]. They also related the fatigue behavior to the fiber stress in the $0°$ ply as in the previous study [3].

Mall and Portner investigated the fatigue behavior of the cross-ply laminate, SCS-6/Ti-15-3 at 427 °C [7]. This study was performed to examine the damage initiation and progression in this material at the elevated temperature. The fatigue tests were all performed in load control mode under the tension-tension loading condition with a load ratio of 0.1 and at two frequencies of 0.02 and 2 Hz. Damage was monitored throughout the test by acetate edge replication and quantified in terms of the initial modulus and the value of the modulus during the test. They found that the two different frequencies had different strains at failure which indicated two different modes of failure. For the high frequency test, brittle cleavage fracture of the matrix was the dominant influence on specimen failure. Cleavage fracture occurs when a crack follows a preferred crystallographic plane along the grains. At high frequency the material tended to strain harden. For low frequency tests, which were exposed to the high temperature for longer periods of time, the fibers failed prior to matrix failure. The matrix age hardened significantly.

Newaz and Majumdar investigated crack initiation in a unidirectional laminate of SCS-6/Ti-15-3 with a center hole [8]. Their purpose was to characterize the crack initiation and crack growth from the holes, as well as determine the crack initiation sites and whether the cracks were through-the-thickness cracks. The fatigue tests were stopped prior to failure for sectioning and polishing so that metallographic examination could be performed. They found that the fatigue loaded specimens developed four major cracks around the periphery of the hole. These cracks were through-the-thickness matrix cracks, and they bridged the fibers. Newaz and Majumdar used the Hencky-Von Mises distortion energy theory to predict the point around the hole where yielding would begin. The major cracks formed between 65° and 72° from the loading axis, which was accurately predicted from the Hencky-Von Mises yield criterion. It is believed that the initiation is controlled by the local inelastic strain of the matrix [9]. They also performed several monotonic tensile tests using the same material and the same notch condition. These specimens developed cracks 90° from the loading axis. They determined that the monotonic specimens failed due to fiber failure while the fatigue tested specimens failed due to matrix failure.

Naik and Johnson investigated the damage initiation in notched SCS-6/Ti-15-3 using the laminate lay-ups of [0]8, [0₂/±45]₂, [0/±45/90]₂, and [0/90]₂s [10]. Some specimens contained center holes while the others contained double edged notches. Two different types of loading were used on these tests. The first type was a constant amplitude load over the life of the entire specimen. The second type was an incremental approach. In this type of loading, the specimen is fatigued for 50,000 cycles at one load

level and then 50,000 cycles at the next higher load level. One of their conclusions was that debonding and matrix cracking served to reduce the effect of the stress concentration. They observed only matrix cracks and no fiber cracks. They also noticed that the heat treated specimens and the as fabricated materials behaved in a similar manner.

Boyum investigated the fatigue behavior of unnotched cross-ply, SCS-6/Ti-15-3 at room temperature under both tension-compression and tension-tension loading [11]. She compared the results of tension-compression at room temperature fatigue testing for the cross-ply layup with the tension-tension at room temperature results. It was found on a maximum applied stress basis as well as an effective strain range basis that the tension-compression specimens had shorter fatigue lives than the tension-tension specimens, and this was caused by the additional damage and plasticity sites which existed only in the tension-compression load case. Along with the room temperature fatigue testing, she also studied the high temperature fatigue behavior (427°C) under tension-compression. The effective strain range was found to be a good parameter for comparing fatigue lives under different loading conditions.

As indicated in this chapter, extensive experimental studies into the fatigue characteristics of the SCS-6/Ti-15-3 composite system have been accomplished. As a result, fatigue life maps of the material under many different loading environments are now available to designers. However, not only is understanding the fatigue life important, but the remaining or residual strength of the material after undergoing specific numbers of cycles or types of loadings is also critical. Aerospace structures and their components follow the strict maintenance and replacement schedules. A single critical component

8

failure may result in catastrophic failure of the total system. Therefore, it is essential to know the strength characteristics of the component at a given time and be able to project when the component must be replaced. In spite of its importance, very little residual strength characterization data are available for titanium MMCs. Such experimental data and analysis techniques are necessary if these materials are to be safely used in real applications. Thus, the present study represents the first step in this direction.

Several experimental works have observed the reduction of the elastic modulus in the loading direction during fatigue of the polymeric composites [12]. In fact, some researchers have attempted to relate the modulus degradation to the interior damage [13]. Sufficient evidence that stiffness change is an indicator of damage in composites has indeed been established by Gottesman, Hashin, and Brull [14].

One obvious condition promoting damage in titanium matrix composites is the mismatch of coefficient of thermal expansion (CTE) between fiber and matrix. However, it has been pointed out by Gabb *et al.* [15] and Mall *et al.* [16] pointed out that the specimens subjected to 10,000 thermal cycles (from $300^{\circ}C$ to $500^{\circ}C$) under zero load did not exhibit degraded mechanical responses during tests. However, owing to the thermal expansion coefficients of the constituents of the composite differing substantially, and because the volume fraction of the fibers is about 0.35, thermal residual stresses that develop during cooling from the processing temperature can have a decisive effect on the deformation of the composite. Fiber deformation is purely elastic, recovery of the composite strain is possible by annealing the deformed composite after unloading. The fibers recover their original shape elastically, inducing reverse creep in the matrix. This

so-called " rejuvenation " was experimentally observed by Khan *et al.* [17] and McLean

[18].

3. *Material, Specimen, and Test Procedures*

3.1 Specimens Descriptions

The material studied in this investigation was a titanium matrix composite. The titanium metal matrix is reinforced with continuous Silicon Carbide (SiC) fibers to form various composite layups. The present study examines unidirectional, $[0]_8$, and cross-ply, $[0/90]_{2s}$ lay-ups. Each layup contained a total of 8 plies. The SiC fibers were made by Textron, under trade name of SCS-6. These fibers were manufactured by chemical vapor deposition (CVD) on carbon core filament. An outer coating was applied to the SiC fiber to protect the inherent surface defects resulting from the CVD proc͏͏͏s and to enhance the abrasion resistance and compatibility with the titanium matrix, and this coating was composed of an overlay of carbon-rich nonstoichiometric amorphous SiC on top of amorphous carbon [19]. The unidirectional or cross-ply fiber mats were made from fibers (with certain interfiber space), binder, and molybdenum (Mo) wires used to cross-weave the SiC fiber in the desired position. The nominal chemical composition of the titanium matrix, Ti-15 3 in weight percentage is shown in Table 1. The constituents properties of the composite material are given in Table 2 [20]. It was produced by hot isostatic pressing (HIP) by placing alternating layers of fibers and thin matrix foil.

The specimens were originally cut from the as received rectangular plate. The specimen edges were then polished to remove any damage from cutting. Also, the unidirectional specimens were cut in a dogbone shape to ensure failure within the gauge section.

Table 1. The Chemical Compositions of the Titanium Metal Matrix, Ti-15-3

constituent	percentages (%)
V	15
Cr	3
Sn	3
Al	3
O	0.13(max.)
N	0.03(max.)
C	0.03(max.)
H	0.015
Fe	0.3(max.)
Ti	Remaining

Table 2. Material Properties of Fiber & Matrix at 427°C

Property	Fiber (SCS-6)	Matrix (Ti-15-3)
Modulus, E (GPa)	440	80
Yield Stress (MPa)	800	525
Coefficient of Thermal Expansion, α (10^{-6} /° C)	4.9	10
Poisson's Ratio, ν	0.25	0.36
Ultimate Strength, σ_{ult} (MPa)	3550 (approx.)	865

A sketch of the unidirectional specimens as shown in Figure 1. The cross-ply specimens were cut into rectangular coupons with the dimensions as shown in Figure 2.
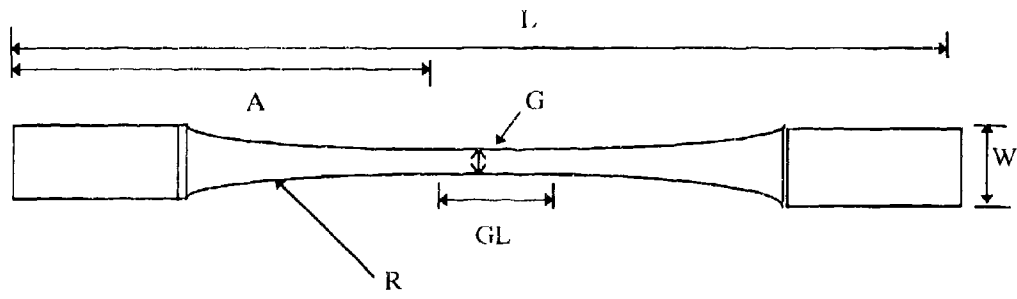
L = 15.2 cm	A = 6.97 cm
GL = 1.27 cm	R = 116 cm
W = 0.9 cm	G = 0.18 cm

Figure 1. Geometry of Dogbone Specimens

A pictorial view of the cross-ply is demonstrated in Figure 3. The average curvature of test specimens was 1160 mm (45.7 in.). All specimens were machined using a diamond encrusted blade and then wrapped in titanium foil and heat treated at 700°C for 24 hours in an argon atmosphere to produce a stabilized matrix microstructure by precipitating out the α phase (i.e., stabilize the microstructure of the matrix material). This heat treatment has also been shown to reduce the residual stress produced during fabrication [1]. The as-received titanium alloy is a metastable, beta (β) phase alloy.
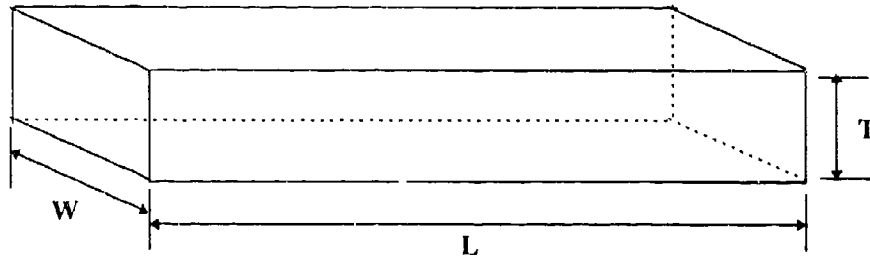
L: 15.2cm(Length),

W: 0.7cm(Width),

T : 0.20cm(Thickness)

Figure 2. The Geometry of Cross-Ply Specimens
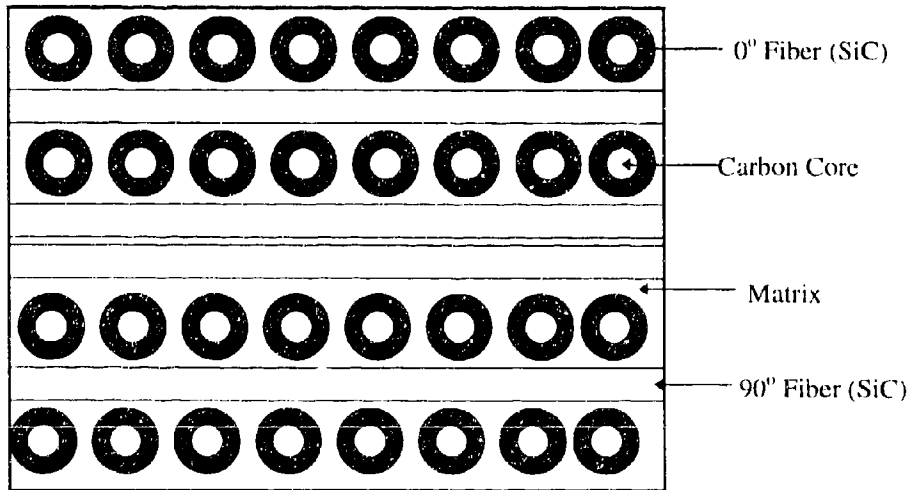
Figure 3. Side View of Cross-Ply Laminate

14

3.2 Test Set-up

Before the fatigue test was started, the alignment of the specimen was ensured to get pure axial loading. The fatigue tests were conducted with a minimum / maximum load ratio (R) of 0.05. Fatigue testing was conducted on a servo-hydraulic test machine under load controlled mode. This was on the 810 Material Test System (MTS 810) as shown in Figure 4 with a 5 Kips load cell which was configured with water-cooled hydraulic grips. A quartz rod, air-cooled, extensometer was used to measure the displacement over the gauge length of 0.5 in. (12.7 mm). The elevated temperature (427°C) was controlled by two 1,000 W, tungsten filament, water-cooled, parabolic strip lamps located on each side of the specimen. The tests were performed using load control under isothermal (427°C) conditions with a load ratio (or stress ratio) of 0.05, and frequencies of 10 Hz and 5 Hz. The mechanical load was applied with a trianglular waveform as shown in Figure 5. The fatigue test profile was obtained from a Zenith 433D computer through a program called "loadtest" developed at the Materials Directorate, Wright Laboratory. The profile for the test included the maximum stress to be reached, the stress ratio, R, specimen area, A, loading frequency, f, temperature, T, *etc.*

Before running the tests, all the specimens were tabbed in the grip area with the aluminum plate (25mm × 7.52mm) through an epoxy adhesive. This required the specimens to be heated to 162°F for 2 hours in order to cure the adhesive. Three thermocouples were welded on the surface of each specimen inside the gauge sectic

15
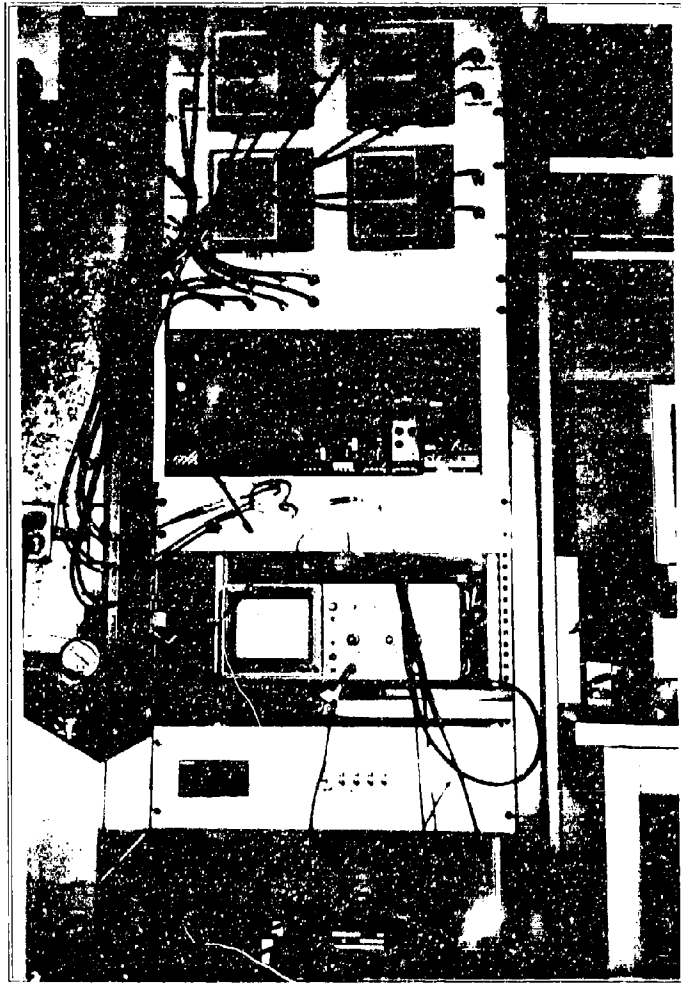
Figure 4. Material Test System Set up (MTS 810)
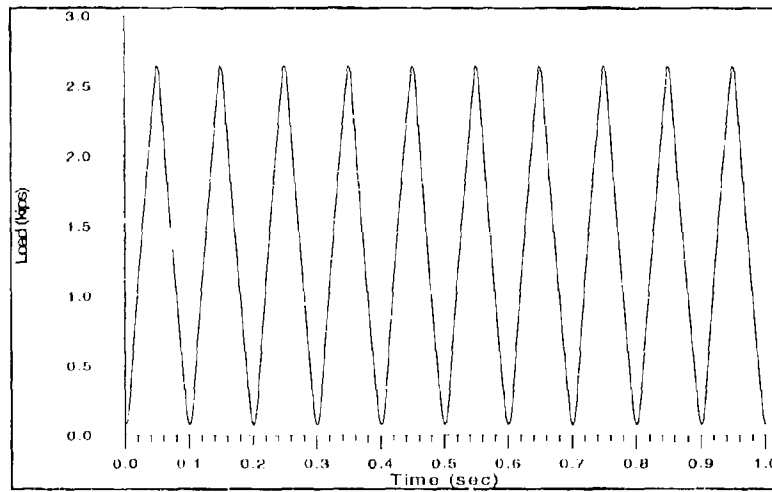
Figure 5. Load Time History for Unidirectional Laminates, Frequency (f)
=10Hz, R=0.05, σ_{max}=900MPa, at 427°C

The position of the thermocouples and the quartz lamps in relation to the specimen during the tests is shown in Figure 6. One thermocouple was mounted directly beneath each lamp, and the third was placed in the center of the gauge section. The displacement, and hence, strain in the gauge section was measured with an extensometer mounted close to the side of the specimen. Two quartz extensometer rods remained in contact with the specimen through a small spring force. See Figure 6 for a picture of the test set-up.

17
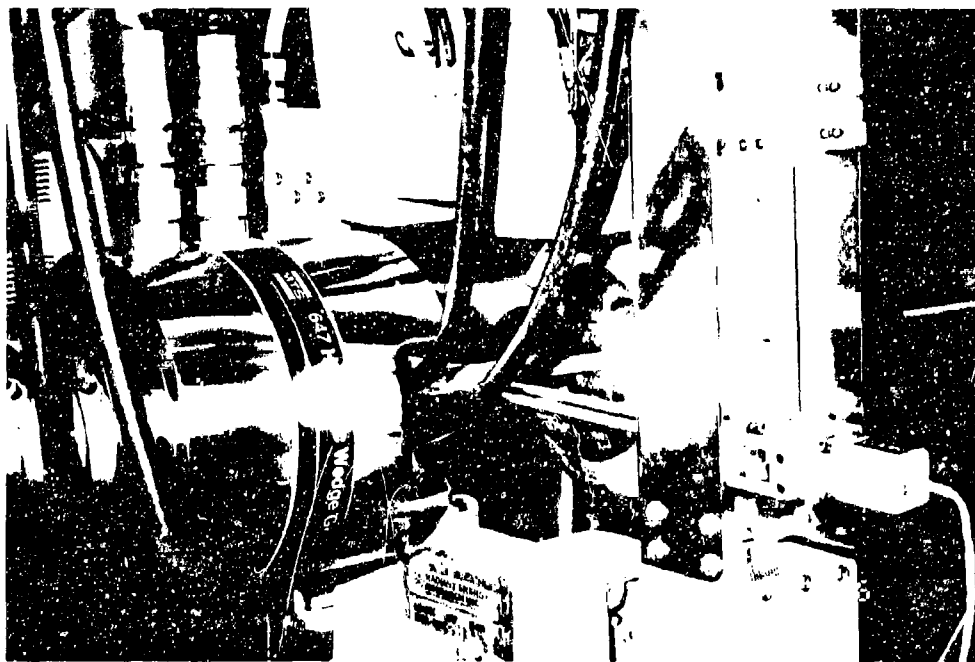
Figure 6. Position of Extensometer on Specimen

3.3 Test Procedures

3.3.1 Unidirectional [0]₁₆ Laminate

Five unidirectional specimens were tested at 427°C with R of 0.05, frequency of 10 Hz, and a maximum stress of 900 MP. First a fatigue test was conducted under these conditions to obtain the failure life (the number cycles to failure) of the unidirectional SCS 6/Ti 15 3. Next, follow on tests were stopped at 25%, 50%, and 75% fatigue life of the first fatigued specimen. These specimens were then loaded to failure at a loading rate of 15 MPa/s to get the residual strength of MMCs. Also, a single specimen with no prior fatigue loading was loaded statically to failure under a 15 MPa/s loading rate to obtain the strength of the virgin material.

At times, extensometer slip occurred during the test. If the extent of the slipping was outside or close to the limits, the test was stopped and the extensometer rods were reset. Upon completion of the test, any displacement data recorded after the slip occurred was shifted to provide a match in the total displacement both before and after the slip.

3.3.2 Cross-Ply $[0/90]_{2s}$ Laminate

Six cross-ply specimens were performed with a frequency of 10 Hz, at maximum stress of 450 MPa, and the other seven cross-ply specimens were conducted with a frequency of 5 Hz, at maximum stress 300 MPa. These tests were conducted under load controlled mode with R ratio of 0.05 at 427°C. The test procedures were the same as that for the unidirectional laminates except that in this case it was important to choose a stress level below the first ply failure (FPF) of the material. The testing results are described in the next chapter.

3.4 Damage Assessment

Three techniques to assess the damage mechanisms were used in this study. They are analysis of fracture surface by scanning electron microscope (SEM), examination of fiber damage away from the fracture area by etching the matrix from the fiber and using SEM, and examination of the matrix and fiber damage away from the fracture area by sectioning and polishing the surface and using an optical microscope.

19

3.4.1 Damage Assessment Preparation

After completing the fatigue and residual strength tests, the half of all specimens were prepared for damage assessment. This was accomplished by cutting the fracture surface off using a diamond cutting wheel, and sectioning the remaining portion of the specimen for polishing and etching as shown in Figure 7.
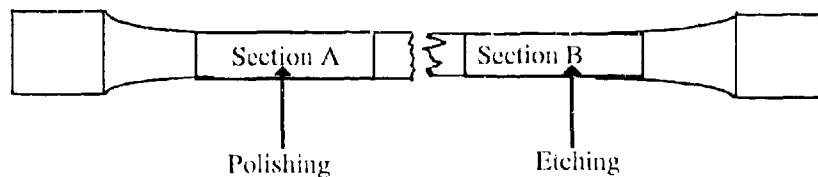
Figure 7. Sectioning of Specimens for Etching and Polishing

3.4.2 Etching Technique

A three percent solution of Ammonium Fluoride and Hydrofluoric Acid (NH_4F + HF) is applied to the specimen to make the first fiber layer appear. This kind of liquid solution can infringe the alpha (α) phase which exists inside the matrix and make α phase precipitate which enables one more easily to observe the slip band (striations), m trix cracking, etc. However, the main reason for etching in the present study was to evaluate the fiber cracking that may have occurred away from the fracture surface. Etching away the matrix was considered a more accurate method of evaluating the amount of fiber damage because it is likely that the act of the polishing may induce additional cracks within the fibers.

20

3.4.3 Polishing Technique

The other part of sectioned specimens were mounted in Buehler Konductimet, a conductive mounting compound, using a Simplimet mounting Press. The first step in the polishing was to use the magnetic wheel with diamond disks for fine grinding, rough polishing, and medium polishing. Each of these steps required 30-40 seconds to complete. This was followed by 15 μm diamond paste on 3 × 5 in. glass plate combined with extender hand polished in a figure 8 manner for 3-4 minutes. Next, the mounted section was then placed on a Buehler Vibromet vibrating polisher with metadi extender in a 1 μm diamond slurry for 2 hours and then the mounted sections were transferred to a Teximet with 1 μm diamond slurry for overnight polishing. At last, the mounted sections were passed on to the Mastermet for 2-3 hours with an aggressive chemical polish which removed all scratches larger than 0.06 μm. After all the mounted section specimens had been polished, they were ready for examination under an optical microscope. The purpose of this examination was to observe the cracks within the matrix or fibers, debonding between the fibers and matrix interface, *etc*.

3.4.4 Fracture Surface Analysis

The fracture surfaces were investigated by Amray 810 scanning electron microscope (SEM) system to observe the damage of the fracture surface which included the microcracks of the matrix, dimple (or ductile) failure for matrix, debonding of fiber-matrix interface, and fiber cleavage (or brittle) failure.

3.4.5 Fiber & Matrix Damage Analysis

The etched sections were used with SEM to observe the fiber or matrix damage. The polished sections were used with the optical microscope for the same purpose of examining the fiber and matrix damage. Both techniques were employed to ensure reliability and to evaluate the most appropriate technique for damage observation.

4. *Results*

The objective of this investigation is to study the residual strength behavior at different percents of fatigue life of unidirectional, $[0]_8$, and cross-ply, $[0/90]_{2s}$, SCS-6/Ti-15-3 metal matrix composite laminate at 427^0 C under tension-tension loading with a stress ratio (R) of 0.05, and frequencies of 10 Hz and 5 Hz. Results of each laminate will be discussed separatedly in the following

4.1 Unidirectional Laminate

4.1.1 Macromechanical Response

The unidirectional specimens were cycled at a maximum stress of 900 MPa with 10 Hz using a triangular waveform. The ability of the controller to maintain the max./min. stress throughout the test was examined and any variation in stress was neglible (less than 2 %).

4.1.2 Fatigue Response

The fatigue behavior was initially dominated by creep deformation of the matrix. The specimen failure was a result of either fiber fracture or matrix cracking.

A nonlinear stress-strain response was observed during the first fatigue cycle. Slip bands provided the physical evidence of plastic deformation. It was also verified from the stress-strain response curve during cycling where the linear loading modulus and unloading modulus were equivalent.

When an MMC specimen is subjected to fatigue testing using the load controlled mode, the strain would show a rapid increase at the end of the fatigue life for the matrix-

23

dominated failure mode. The reduction in stiffness suggests that this behavior was the result of fatigue damage (matrix cracking).

Figure 8 and 9 illustrate the stress strain response for the unidirectional laminate under the monotonic loading and cyclic fatigue loading. From Figure 8, it shows that the linear characteristics behavior occurred on these MMCs. Also, for the fatigue loading case, as the applied cycle numbers increases, the permanent strain increases and the modulus of the specimen decreases until failure.
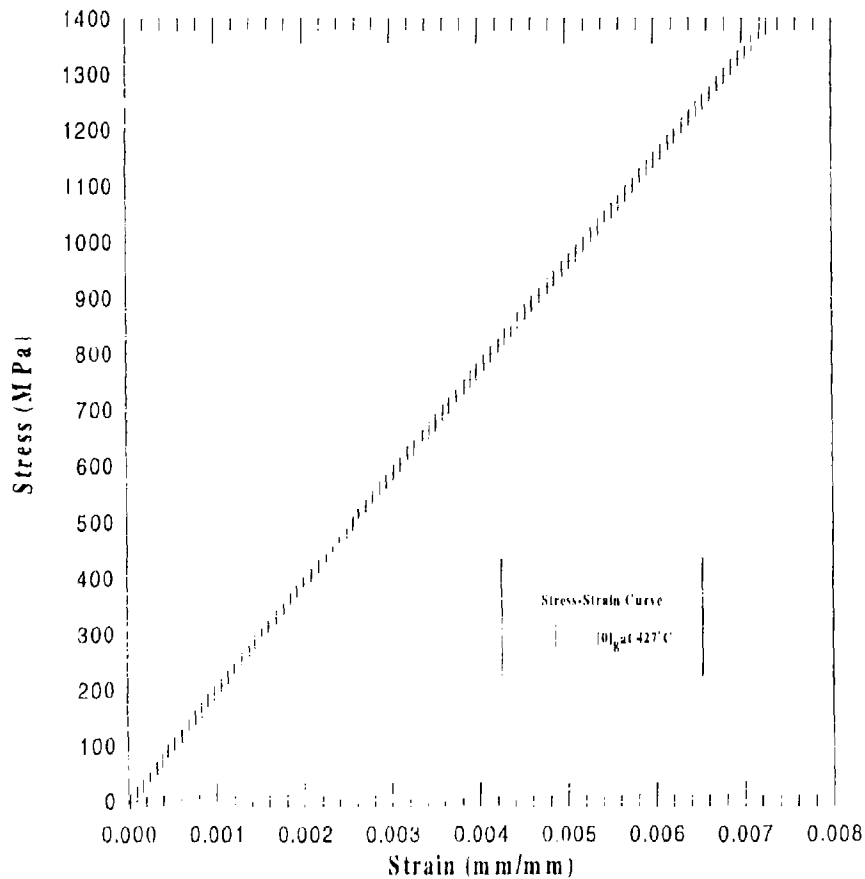
Figure 8. Stress-Strain Response for $[0]_8$ Laminates at 427° C, with a Stress Rate of 15 MPa/s (Montonic Test)
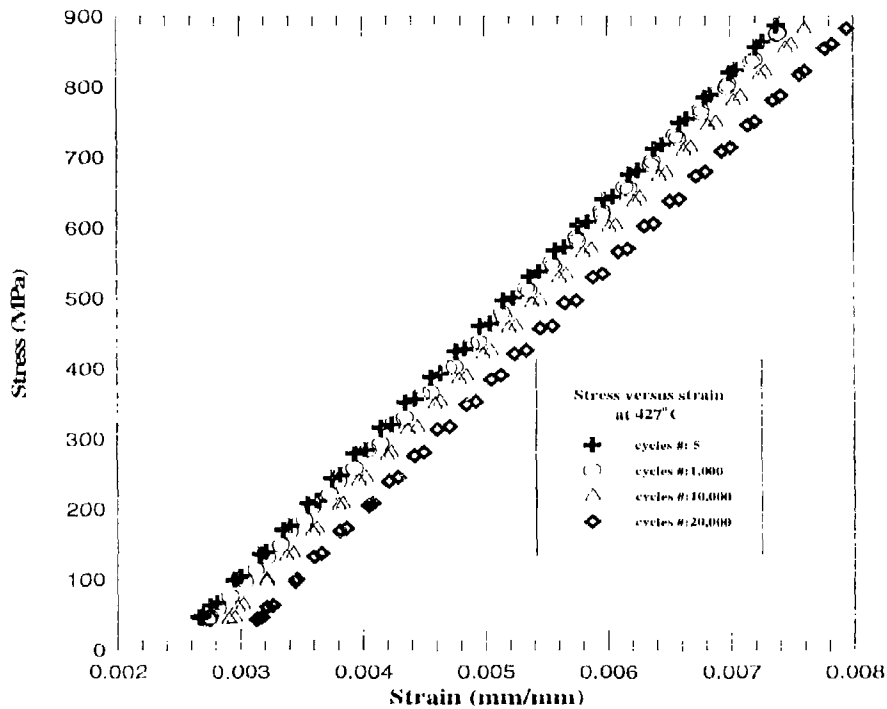
Figure 9. Stress-Strain Response for [0]$_8$ Laminates Fatigue Test at 427°C; σ_{max} =900 MPa, R=0.05, f=10 Hz Conditions

A common consequence of fatigue in composite is a reduction in stiffness which begins very early in the fatigue life. The modulus versus cycles, and normalized modulus versus normalized cycles diagrams are shown in Figures 10 and 11, respectively. The modulus drop is shown to be approximately 3 % over the fatigue life. The normalized modulus is defined as the measured modulus during the fatigue test divided by the initial modulus of the undamaged specimen (i.e., E/E_i). In the same way, the normalized cycle is the measured cycles divided by the fatigue life (i.e., N/N_f).

25
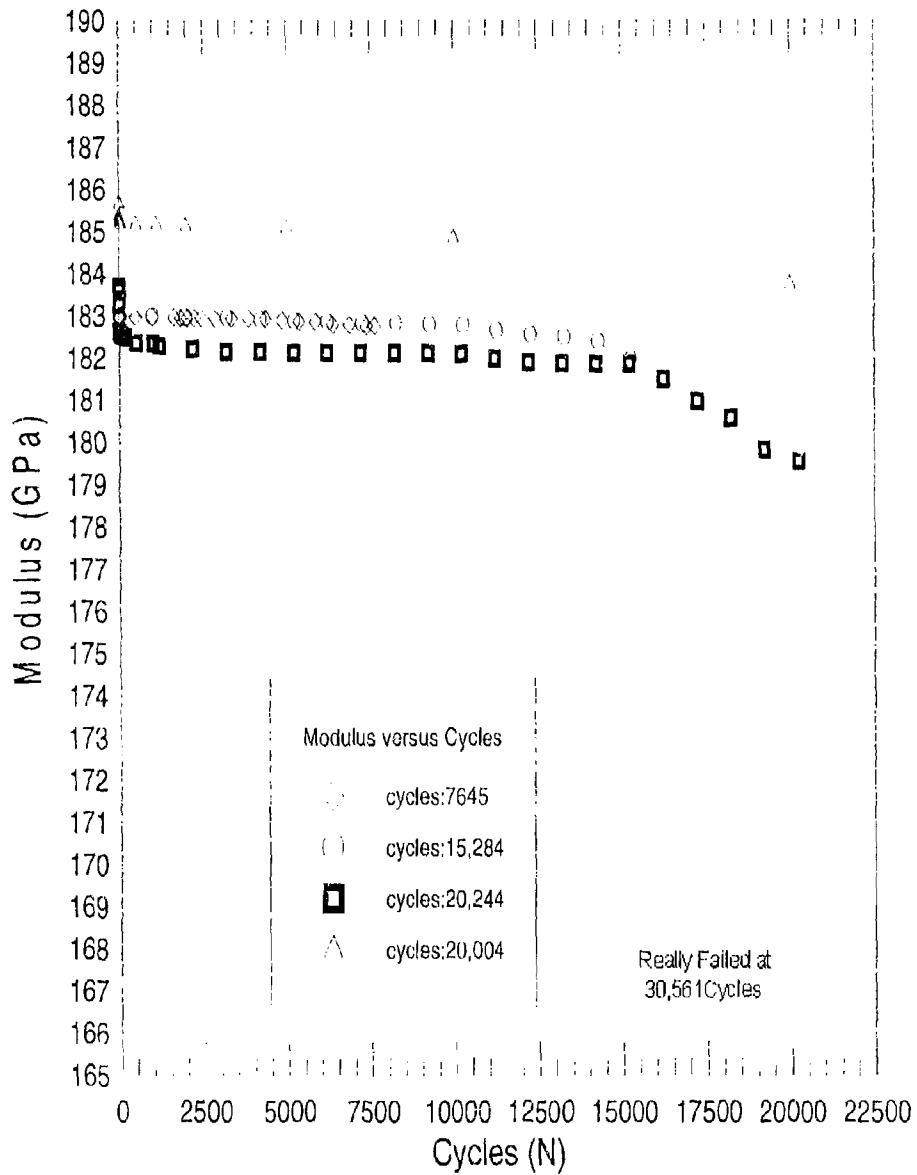
Figure 10. Modulus Cycles Relationship for [0]₈ Laminates under 427°C, σ_{max}=900 MPa, R=0.05, f=10 Hz Conditions
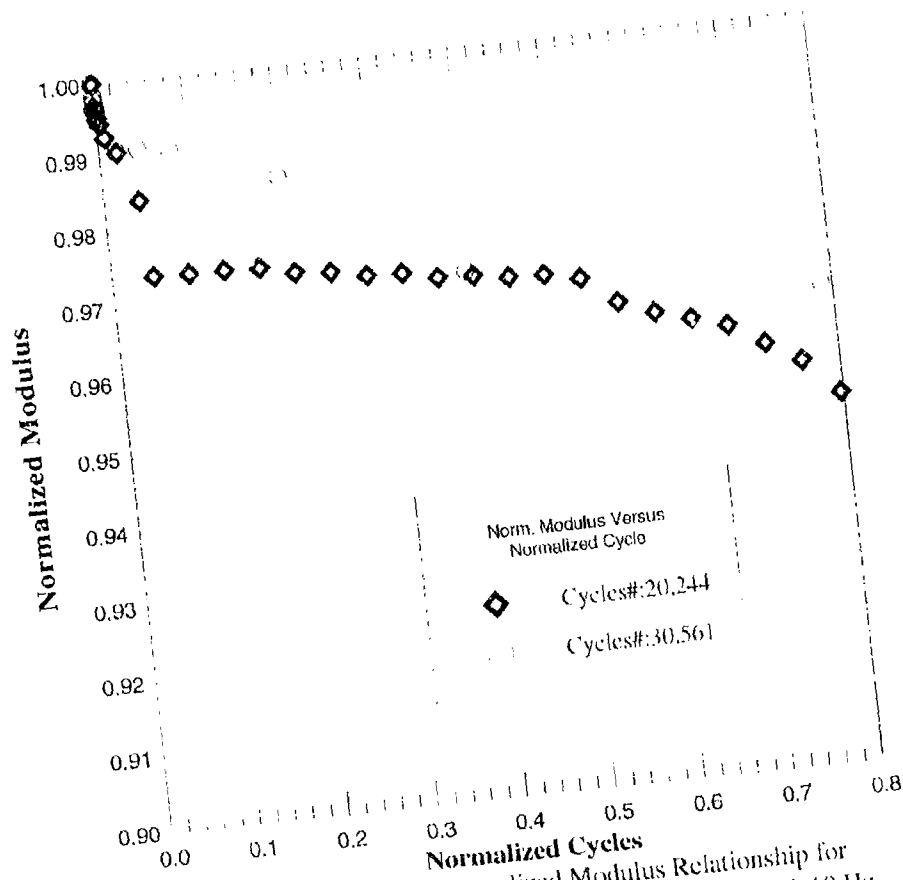
Figure 11. Normalized Cycles vs Normalized Modulus Relationship for [0]₈ Laminates under 427° C, σ_{max}=900 MPa, R=0.05, f=10 Hz

The strain and cycles response for [0]₈ laminates are shown in Figure 12. From these plots, it is apparent that the strain does not change very much before two thirds of the fatigue life (i.e., 2/3 N₁). They also show that the strain suddenly increased just prior to specimen failure.
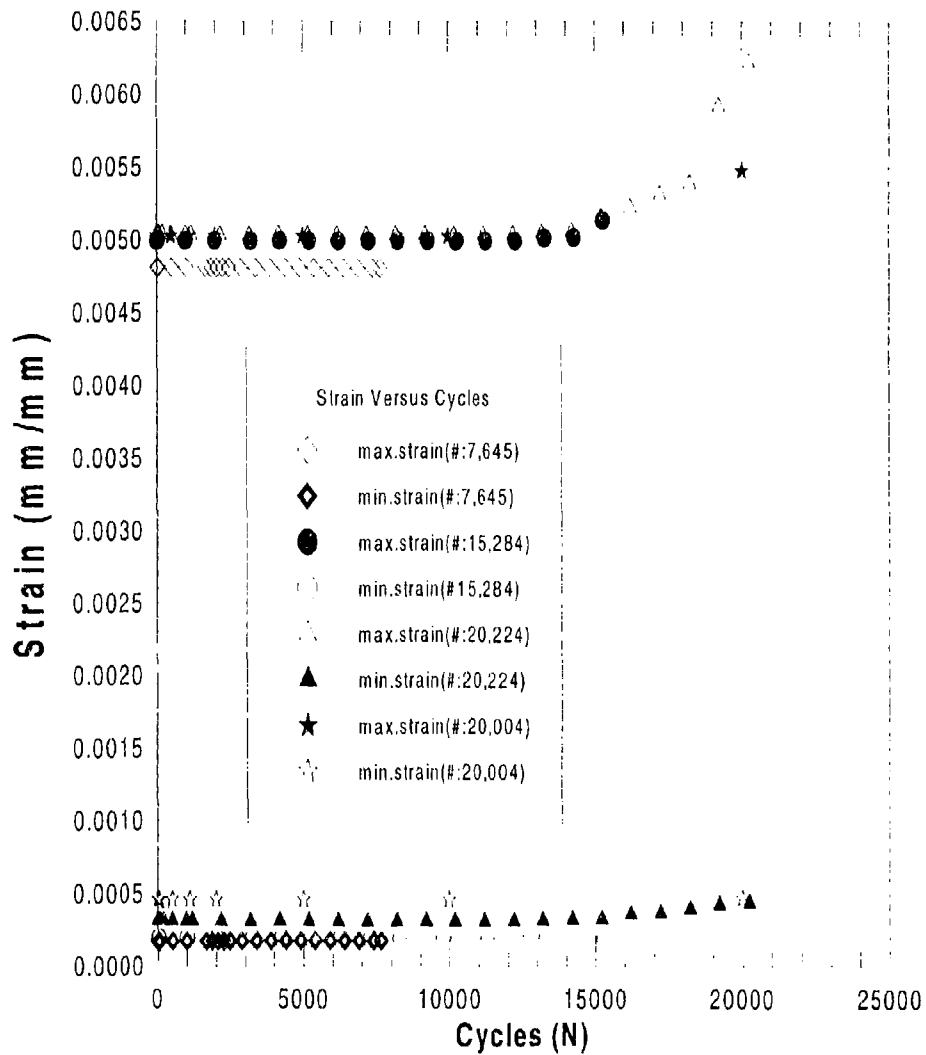
Figure 12. Comparisons for the [0]₈ Laminates Fatigue Tests at σ_{max} =900 MPa, R=0.05, f=10 Hz, 427° C Conditions

The residual strength results of the unidirectional laminates for these tests are shown in Figures 13 and 14, and Table 3. In Figure 13, it is observed that the residual strength of the unidirectional laminate decreases with increase of the applied fatigue

cycles, however, this decrease is very small. Rather than a gradual decrease over the life, the strength of the specimens exhibited more of a catastrophic or critical drop in strength near the end of the life.
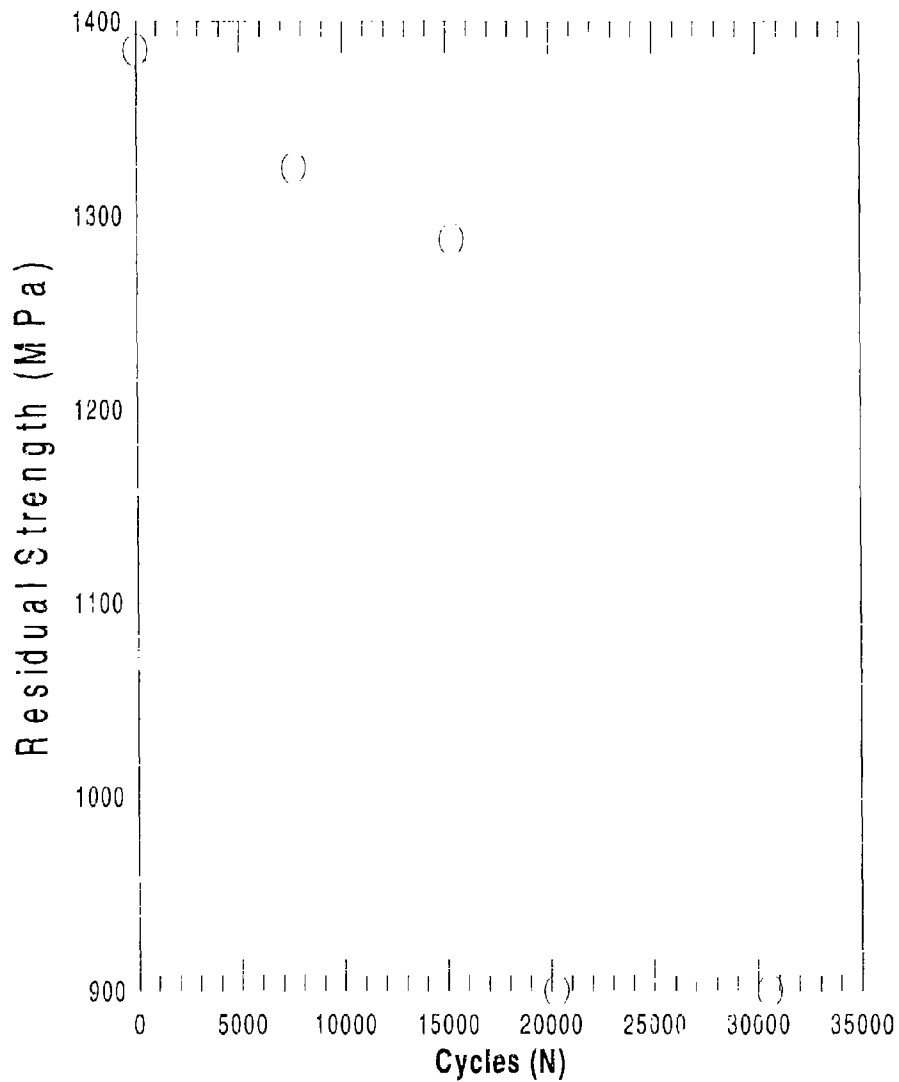
Figure 13. Residual Strength & Cycles Relationship for $[0]_8$ Laminate
at $427^{\circ}C$, $R=0.05$, $\sigma_{max}=900$ MPa, $f=10$ Hz Conditions
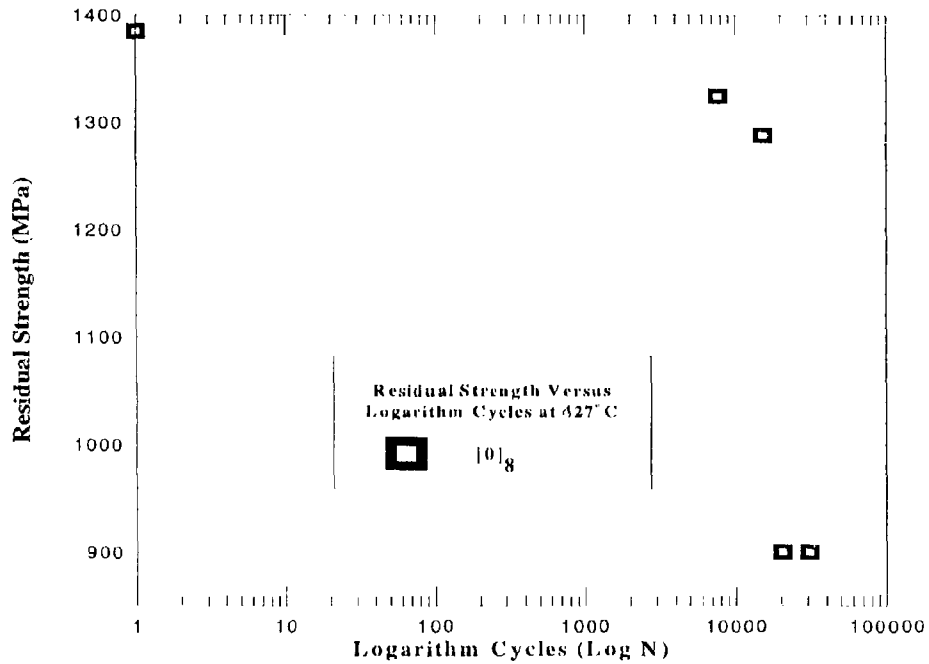
Figure 14. Residual Strength *vs* Logarithm Cycles Relationship for [0]$_8$
Laminates at 427°C, R=0.05, σ_{max}=900 MPa, f=10 Hz

Table 3: Residual Strength Results of [0]$_8$ Laminates & Their Applied Conditions
(σ_{max}=9C0 MPa)

Specimen Type	Load Mode	Cycle Numbers	Area (mm^2)	Max.Strain Change (mm/mm)	Frequ -ency (Hz)	Thermal Strain (mm/mm)	Temp- erature	Residual Strength (MPa)
Unidire- ctional (900MPa)	Static *	0	12.9	. . . . -		0.00224	427° C	1385.7
"	Cyclic	7,645 (25%)	12.92	0.00002	10	0.00226	"	1324.5
"	"	15,284 (50%)	12.91	0.00014	"	0.00226	"	1287
"	"	20,244 (75%)	12.93	0.001085	"	0.00228	"	900 **
"	"	30,561 (100%)	12.92	0.000453	"	0.00222	"	900

* Static test with a stress rate of 15 MPa/s

** Specimen failed before got the residual strength

4.2 Cross-Ply Laminate

4.2.1 Macromechanical Response for σ_{max}=450 MPa

Five specimens of cross-ply lay-up were tested under fatigue to a maximum stress of 450 MPa. These consisted of a fatigue test to failure, and four other residual strength tests to 38%, 40%, 50%, 75% of fatigue life of the first fatigued specimen. After having reached the pre-determined cycle limit, each residual strength specimen was tested under a static load to failure with a stress rate of 15 MPa/s to get the residual strength. All the fatigue tests were performed with an R (minimum load/ maximum load) of 0.05, and a frequency of 10 Hz under 427°C. Two static tests of the virgin crossply materials were also conducted.

The stress strain curve for static loading is shown in Figure 15. It presents the slightly nonlinear characteristics.
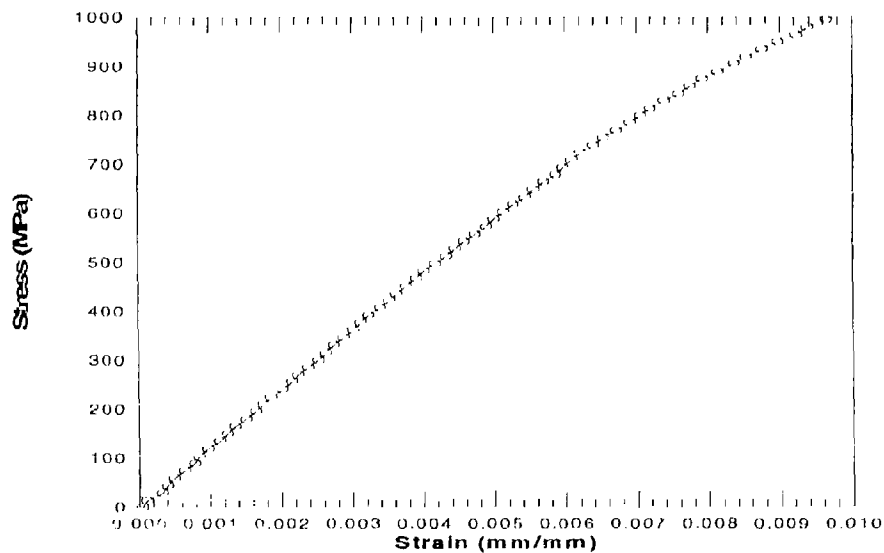
Figure 15. Stress Strain Response for $[0/90]_{2s}$ at 427°C, Stress Rate=15 MPa/s (Static Loading)

31

The modulus vs cycles relationships are demonstrated in Figures 16 and 17. At the beginning of the fatigue test, the modulus decreased slightly, followed by little or no change with increasing cycles until approximately two thirds of the fatigue life, where it continued to drop with increasing cycles.
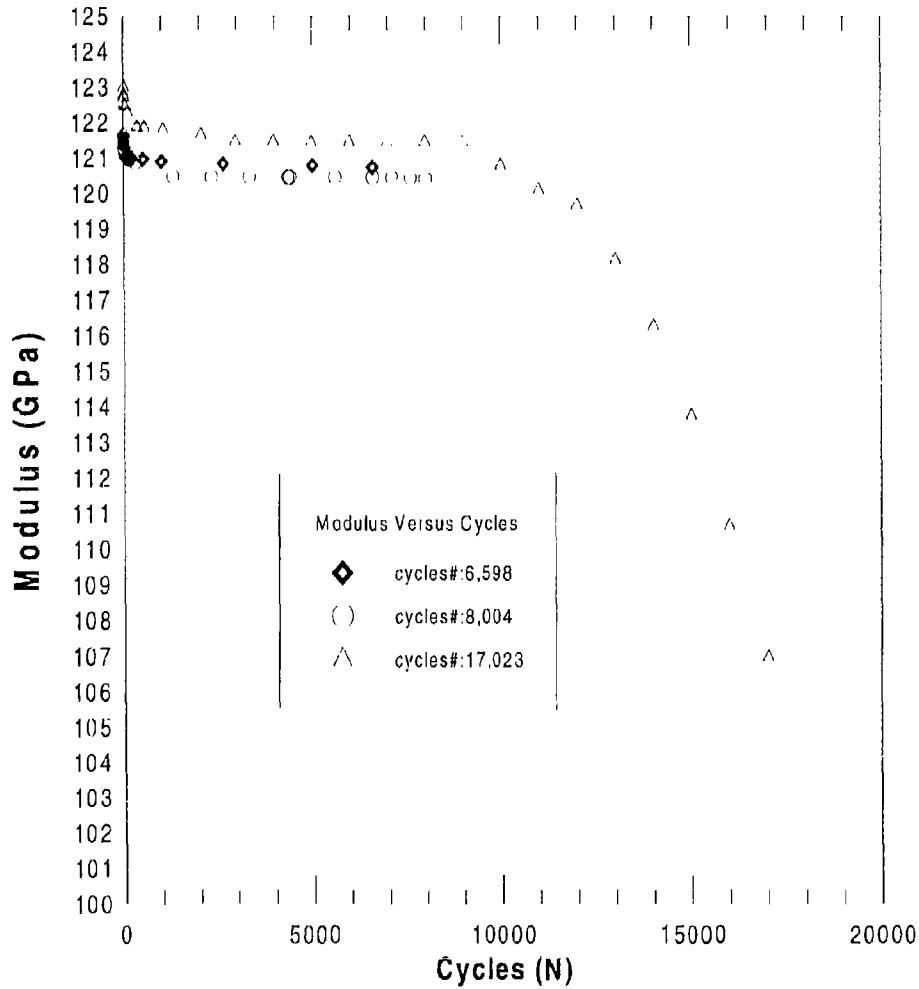
Figure 16. Modulus Cycles Response for $[0/90]_{2s}$ under Cyclic Loading at σ_{max} =450 MPa, R=0.05, f=10 Hz, 427° C
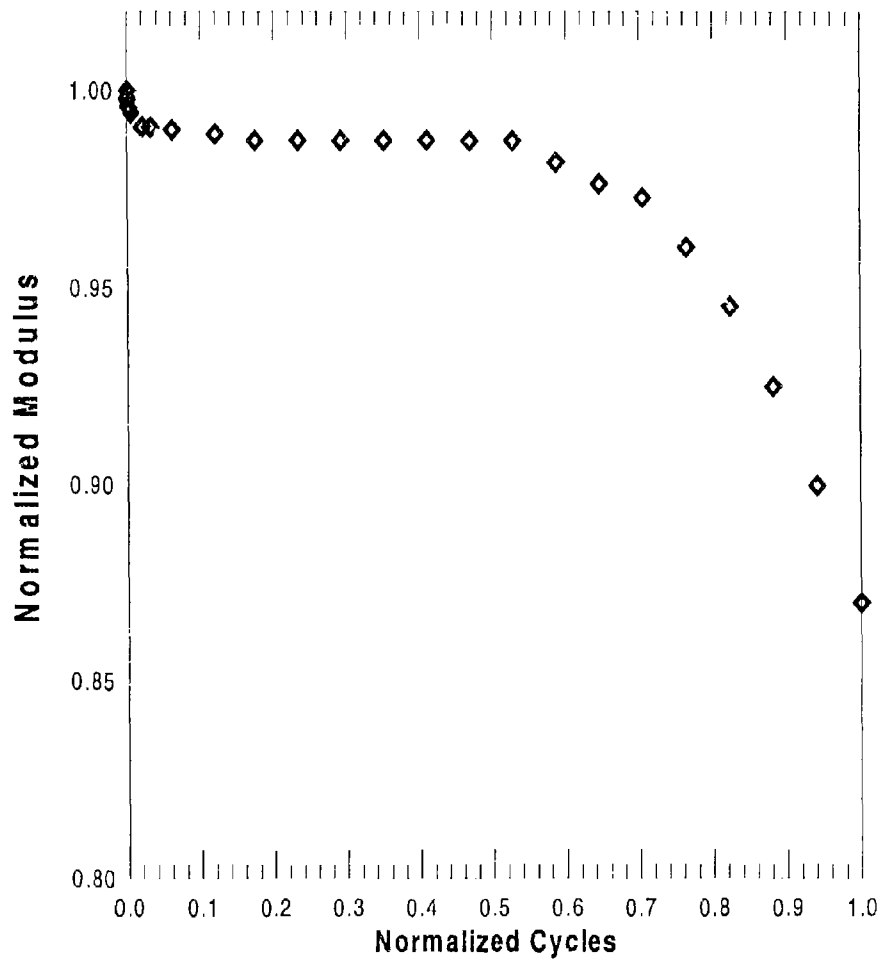
Figure 17. Normalized Modulus *vs* Normalized Cycles Response for |0/90|$_{2s}$
under Cyclic Loading at σ_{max} =450 MPa, R=0.05, f=10 Hz, 427° C

The strain vs cycles are shown in Figures 18 and 19. As it can be seen in these figures, there was a rapid increase in strain over the first few cycles. This may be attributed to viscoplastic deformation of the matrix and was a very short-lived effect. This was followed by a plateau region with a very slow increase in strain to failure.

33
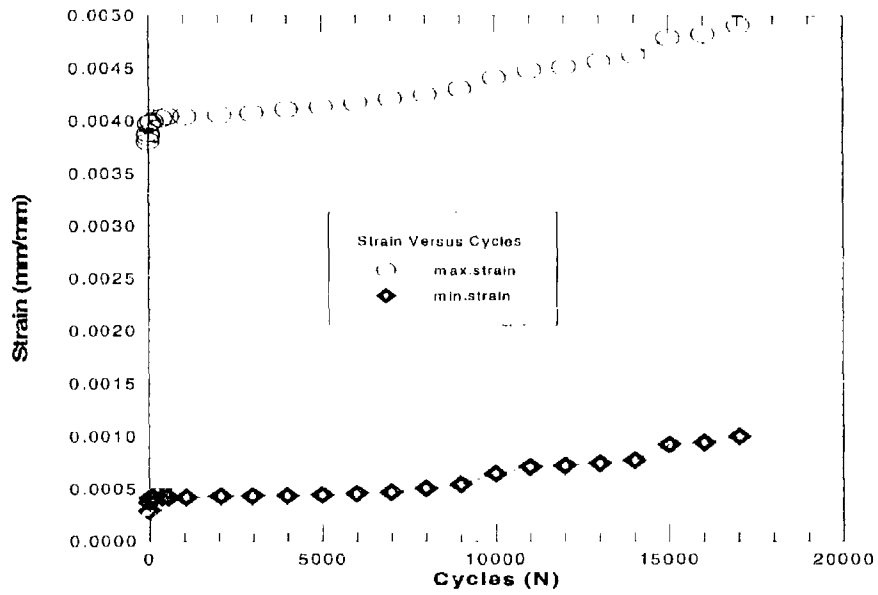
Figure 18. Max.& Min. Strain *vs* Cycles for Fatigue Test at σ_{max} =450 MPa, R=0.05, f=10 Hz, 427° C
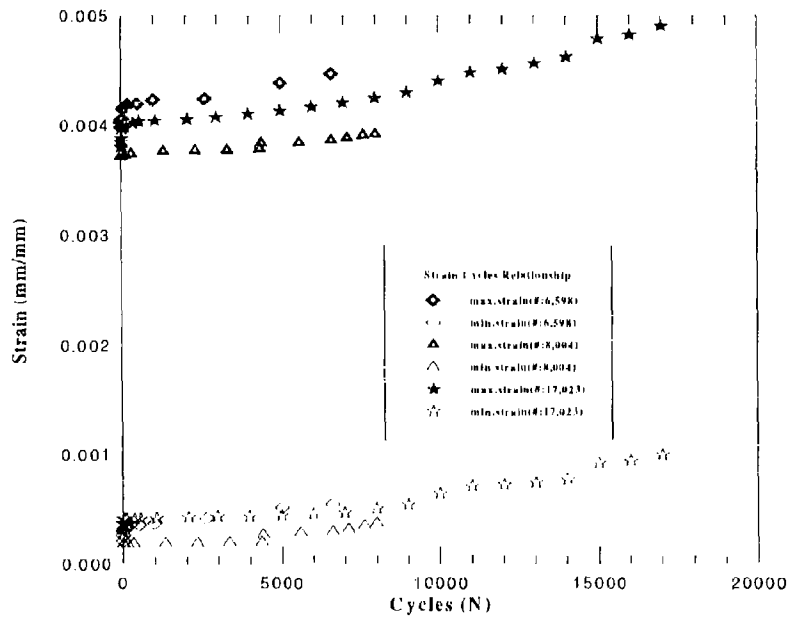
Figure 19. Strain *vs* Cycles for Fatigue and Residual Strength Tests at σ_{max} =450 MPa, R=0.05, f=10 Hz, 427° C

34

The residual strength results of the cross-ply for the specimens fatigued to 450 MPa maximum stress are shown in Figures 20-21, and Table 4.

Residual Streng
Versus Cycles at 427 C

◇ Maximum Stress=450 MPa

Residual Strength (MPa) (y-axis: 400, 500, 600, 700, 800, 900, 1000)

Cycles (N) (x-axis: 0, 5000, 10000, 15000, 20000)
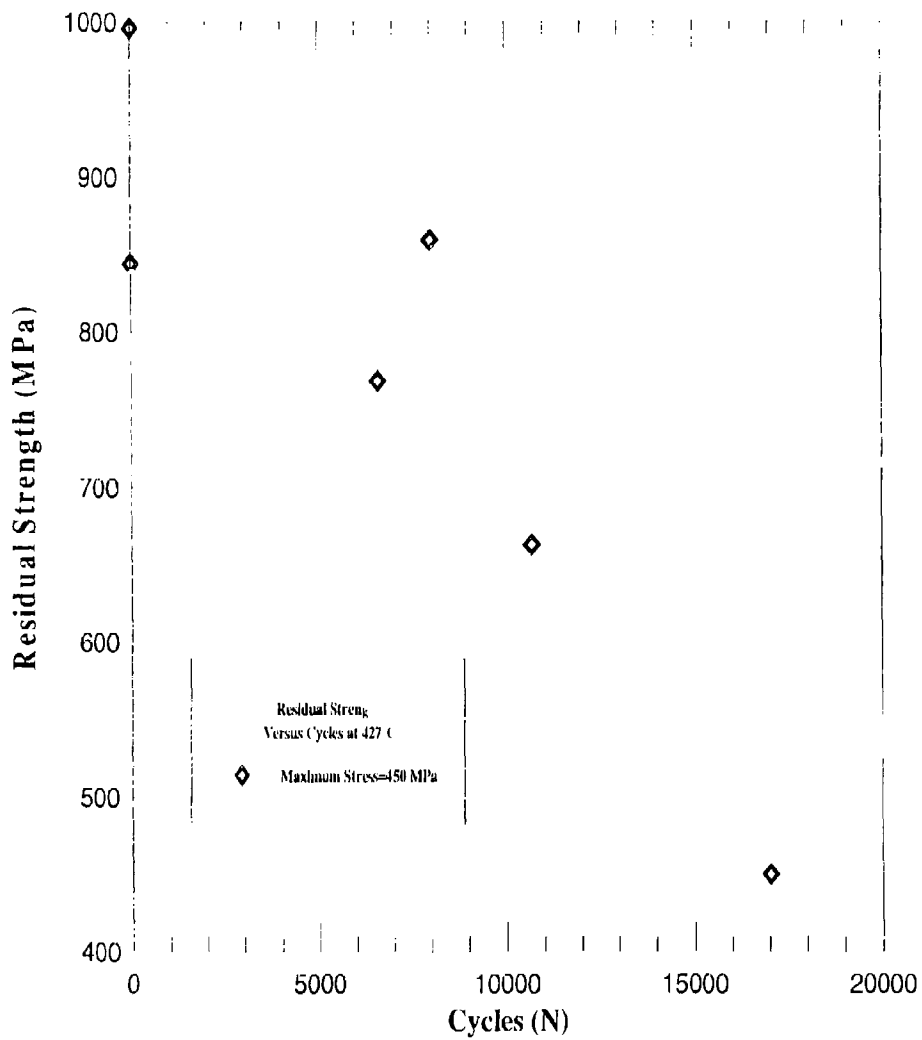
Figure 20. Residual Strength *vs* Cycles for [0/90]$_{2s}$ Laminates
at 427° C, R=0.05, f=10 Hz, σ_{max}=450 MPa
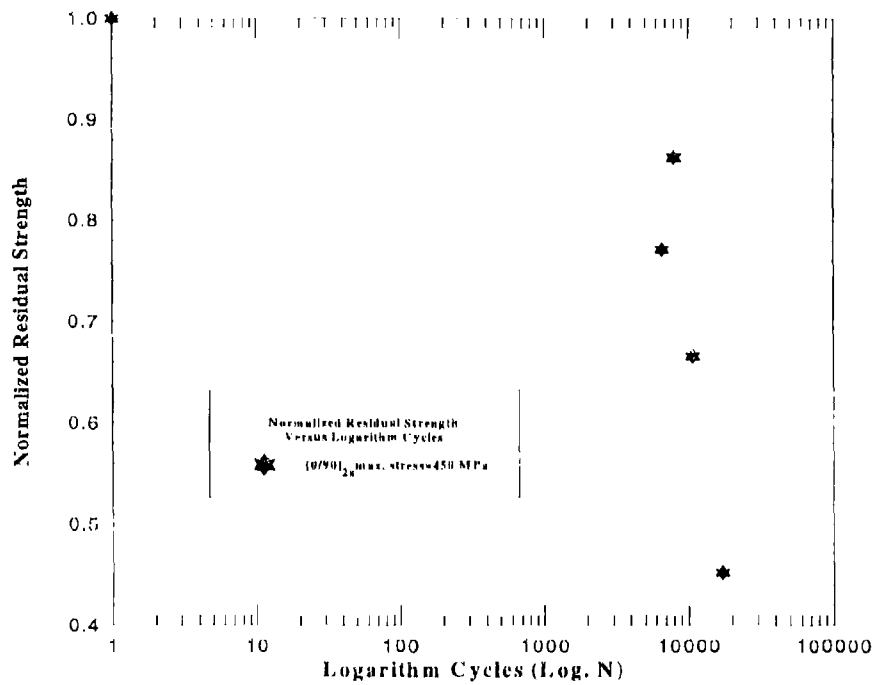
Figure 21. Normalized Residual Strength *vs* Logarithm Cycles for
$[0/90]_{2s}$ Laminates at 427° C, R=0.05, f=10Hz, σ_{max}=450 MPa

Table 4. The Residual Strength Results for $[0/90]_{2s}$ Laminates and Their
Applied Conditions (σ_{max}=450 MPa)

Specimen Type	Load Mode	Cycle Numbers	Area (mm²)	Max.Strain Change (mm/mm)	Frequ- ency (Hz)	Thermal Strain (mm/mm)	Temp- erature	Residual Strength (MPa)
Cross-Ply	Static	0	13.30	---------	0	0.00268	427^{0}C	995.86
"	"	"	13.51	"	"	0.00266	"	843.79
"	Cyclic	6,598 (38%)	13.36	0.00049	10	0.00262	"	768.14
"	"	7,003 (40%)	13.27	0.00062	"	0.00276	"	450 *
"	"	8,004 (50%)	13.60	0.000205	"	0.00274	"	859.2
"	"	10,692 (75%)	13.02	0.00298	"	0.00286	"	662.64
"	"	17,023 (100%)	13.16	0.001014	"	0.00331	"	450

* Specimen failed before residual strength obtained

4.2.2 Macromechanical Response for σ_{max}=300 MPa

Six tests of the crossply material were conducted at a maximum stress of 300 MPa in fatigue. This lower stress level was chosen to determine if the characteristics of the residual strength behavior, as observed previously, were dependent on the maximum stress of the fatigue load.

The maximum strain vs cycles relationships were shown in Figure 22. The strain increased with the increasing cycles.
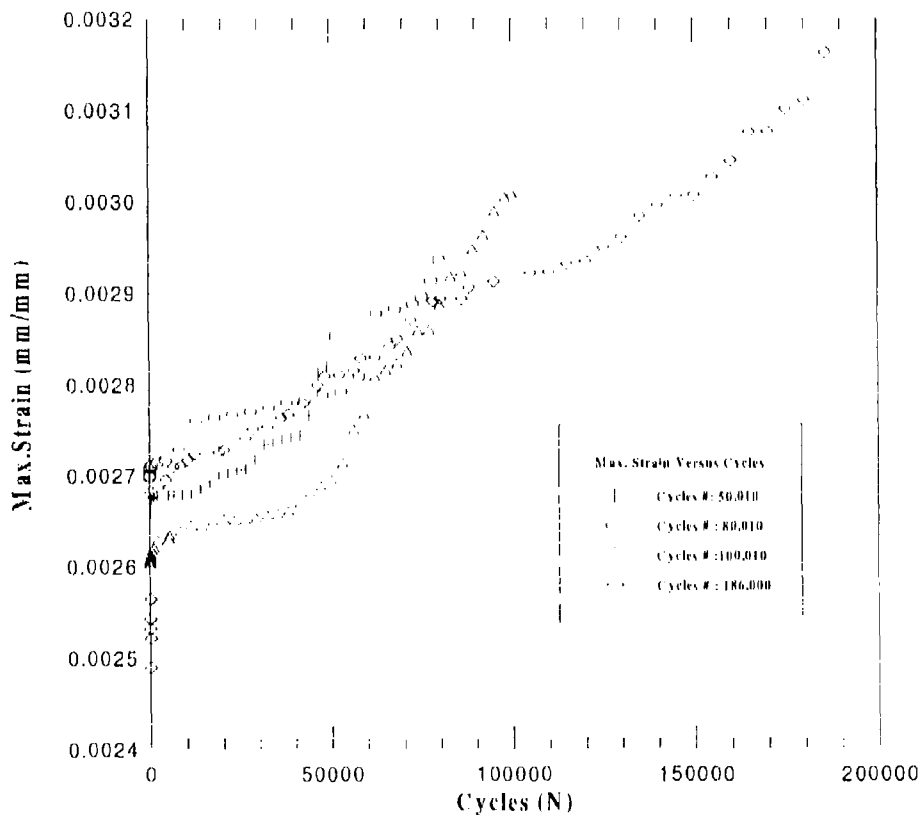
Figure 22. Max. Strain vs Cycles for [0/90]$_{2s}$ Laminates at 427° C, R=0.05, f=5 Hz, σ_{max}=300 MPa

Figure 23 shows the modulus and cycles relationship for these fatigue tests. Also, from these plots, the modulus was found to decrease slowly with cycles in an almost linear fashion until approximately two-thirds of the fatigue life of the first fatigued specimen at which point the modulus dropped more rapidly.
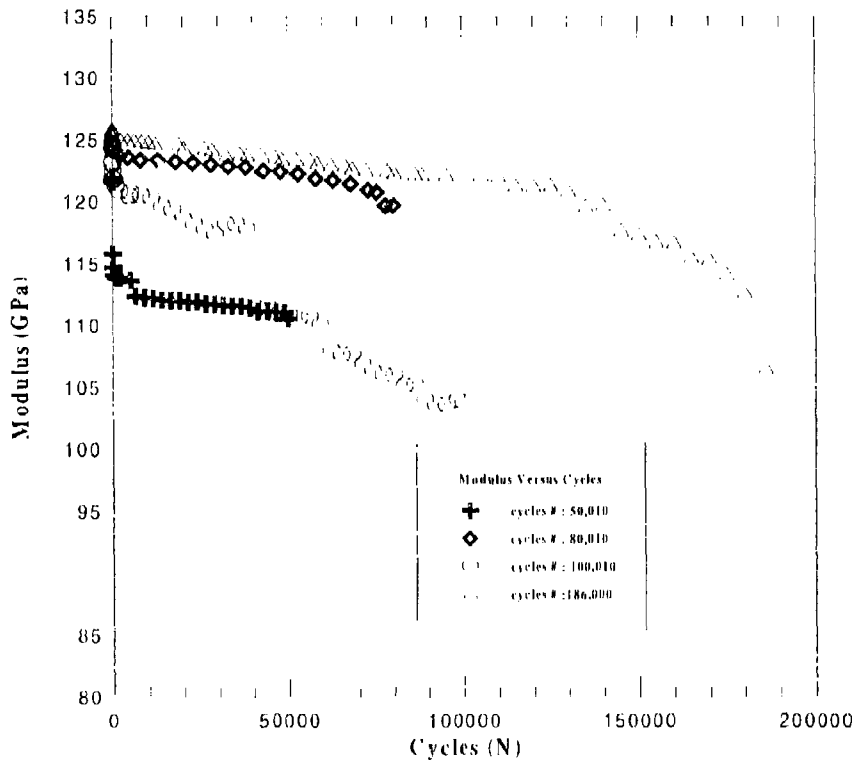
Figure 23. Modulus vs Cycles for $[0/90]_{2s}$ Laminates at 427° C, R=0.05, f=5 Hz, σ_{max}=300 MPa

The residual strength results after different percentages of fatigue life are shown in Figures 24 and 25, and Table 5. These specimens were loaded at a constant stress rate of 15 MPa/s. Two specimens failed before the residual strength could be obtained.
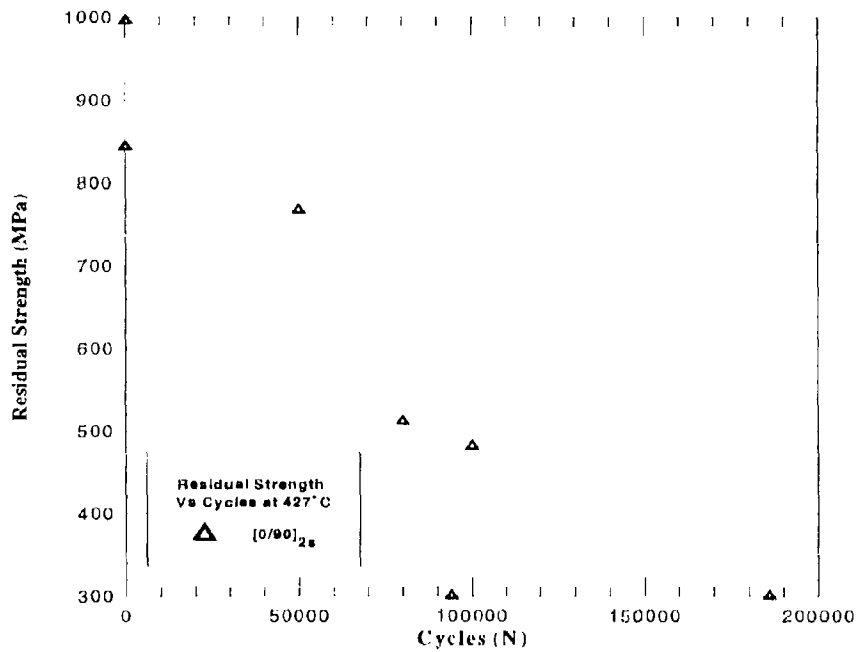
Figure 24. Residual Strength *vs* Cycles for [0/90]$_{2s}$ Laminates at 427° C, f=5 Hz, R=0.05 with a Stress Rate of 15 MPa/s
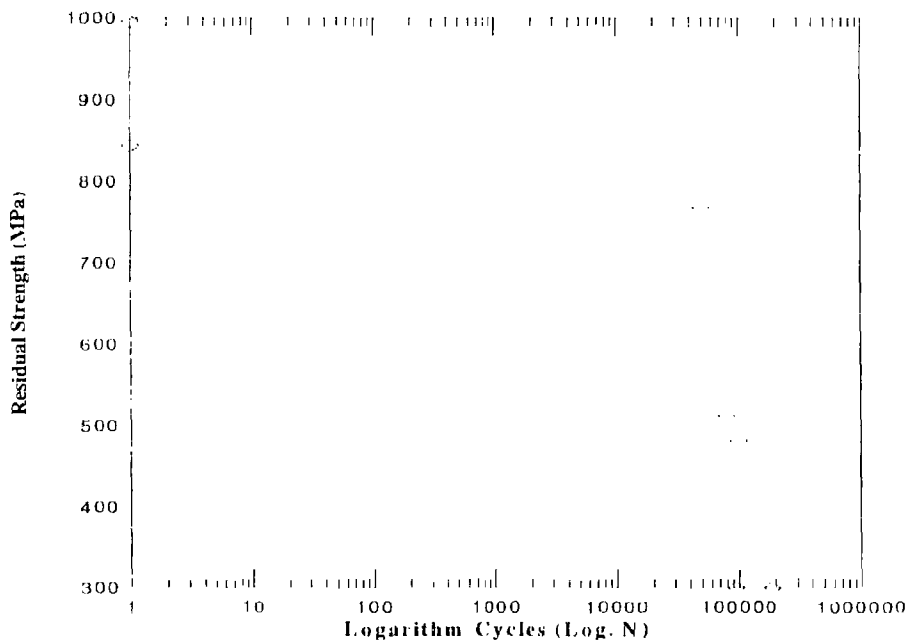
Figure 25. Residual Strength *vs* Logarithm Cycles for [0/90]$_{2s}$ Laminate under 427° C, σ_{max}=300 MPa

39

Table 5. The Residual Strength Results for $[0/90]_{2s}$ Laminates and Their
Applied Conditions (σ_{max}=300 MPa)

Specimen Type	Load Mode	Cycle Numbers	Area (mm²)	Max.Strain Change (mm/mm)	Frequency (Hz)	Thermal Strain (mm/mm)	Temperature	Residual Strength (MPa)
Cross-Ply (300MPa)	Static	0	13.51	----------	0	0.00266	427°C	995.86
"	"	"	13.30	"	"	0.00268	"	843.79
"	Cyclic	50,010	13.33	0.000706	5	0.00266	"	767.17
"	"	80,009	13.53	0.000809	"	0.00262	"	511.62
"	"	94,153	13.24	0.00085	"	0.00278	"	300.00
"	"	100,011	13.32	0.000838	"	0.00264	"	481.20
"	"	186,003	13.00	0.001034	"	0.0030	"	300.00

The comparisons of the cross-ply laminates at different stress level are shown in Figures 26 and 27, and Table 6. Although the fatigue tests were applied at different frequency, the results were very similar for the response of modulus vs cycles and strain vs cycles. In both instances, the modulus didn't change much before two-thirds of the fatigue life or until near the end of the fatigue life; whereas, the strain for $[0/90]_{2s}$ laminates increased gradually with the increasing cycles until near the end of the fatigue life when it increased suddenly.
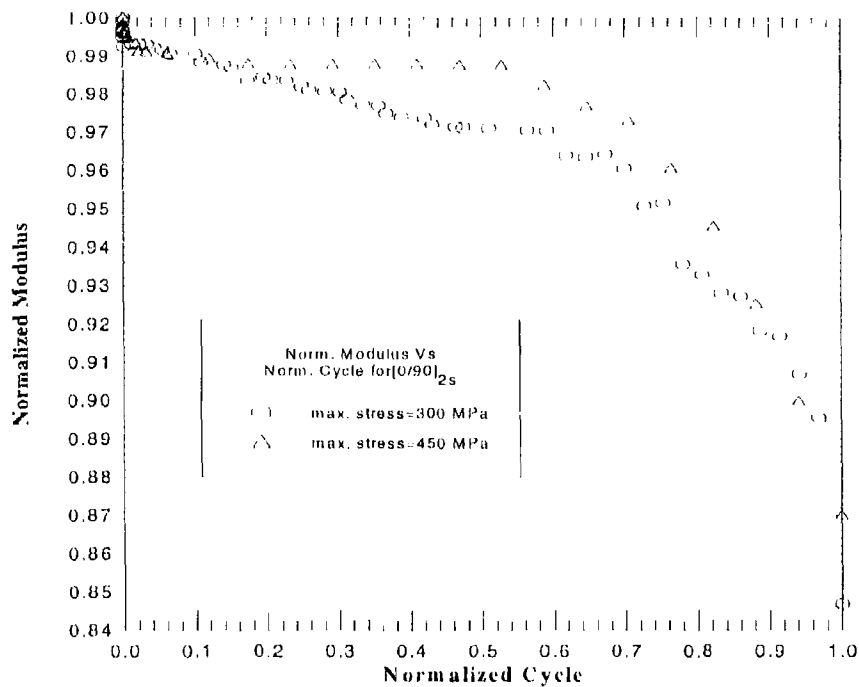
Figure 26. Normalized Modulus vs Normalized Cycle for [0/90]$_{2s}$ Laminates, at 427°C, f$_{300}$=5 Hz, f$_{450}$=10 Hz
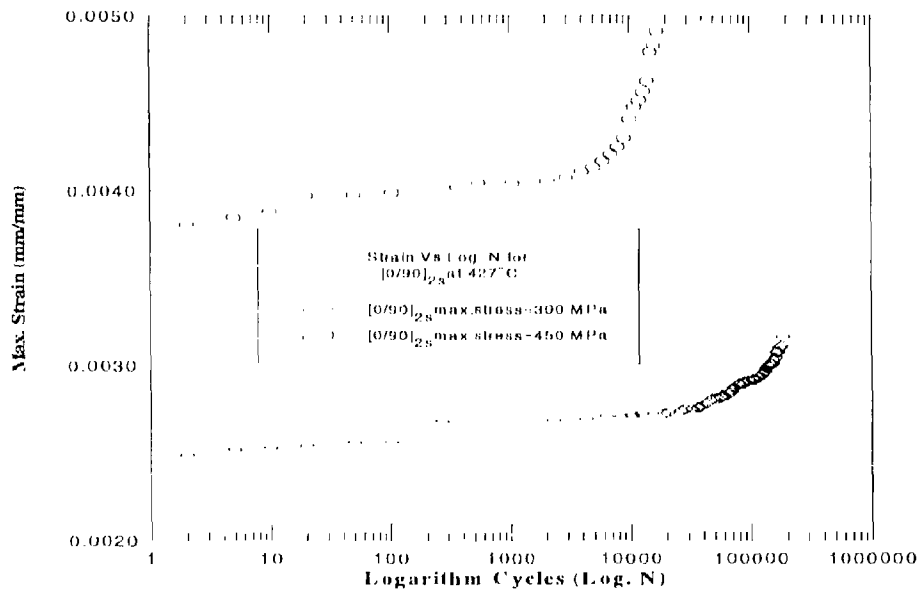
Figure 27. Maximum Strain vs Logarithm Cycle for [0/90]$_{2s}$ Laminates, at 427°C, f$_{300}$=5 Hz, f$_{450}$=10 Hz.

41

Table 6. The Results of the $[0/90]_{2s}$ Laminates at $427\,^{\circ}$ C

Load Mode	σ_{max} (MPa)	Cycles (N)	Frequency (Hz)	Residual Strength (MPa)	$\Delta\,\varepsilon_{max}$ (%)
static	-----	0	0	995.86	-----
"	-----	0	0	843.79	-----
cyclic	450	6,598	10	768.14	0.049
"	"	8,004	"	859.20	0.0205
"	"	10,692	"	662.64	0.0298
"	"	17,023	"	450.00	0.1014
"	300	50,010	5	767.17	0.0706
"	"	80,010	"	511.62	0.0809
"	"	100,010	"	481.20	0.0838
"	"	186,000	"	300.00	0.1034

4.3. Macroscopic Comparisons

This section provides the comparison of all three sets of tests.

4.3.1 Tensile Loading

Figure 28 shows that the modulus of the unidirectional specimen was higher than the cross-ply laminates as is expected.
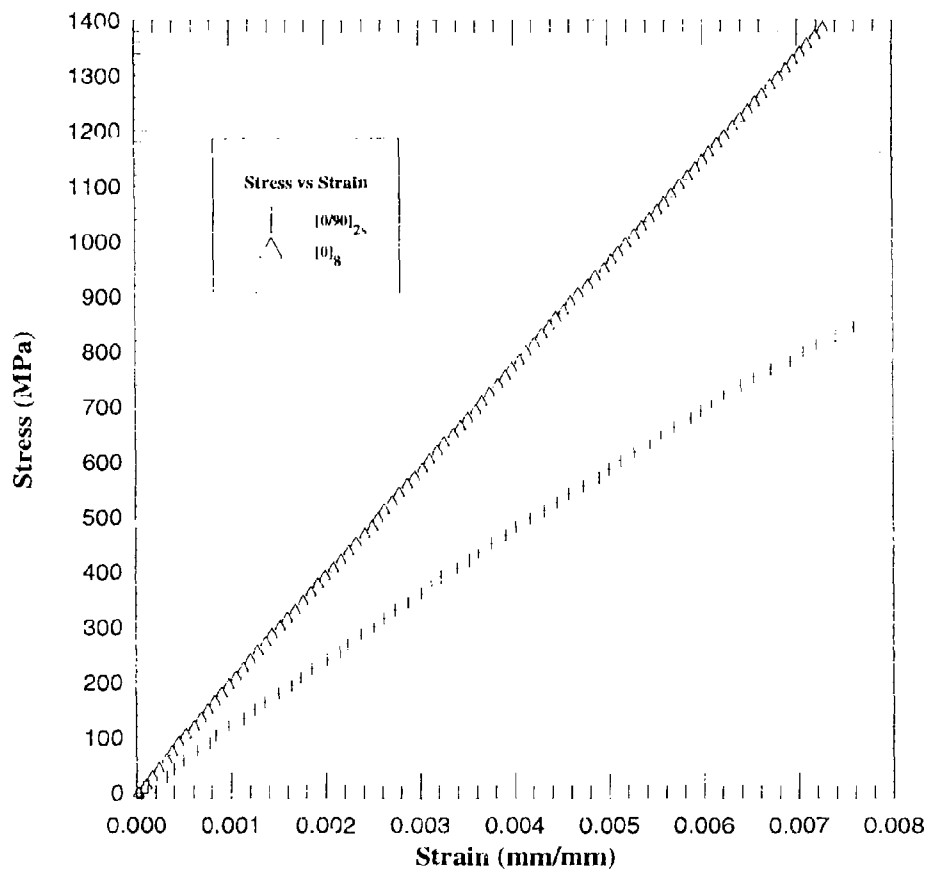
Figure 28. Stress-Strain Relationship of $[0]_8$ and $[0/90]_{2s}$ at 427° C

Figure 29 displays the normalized modulus and normalized cycles relationships for the unidirectional laminates and cross-ply laminates. As expected, cross-ply laminate showed more degradation in modulus than the unidirectional laminate.

43
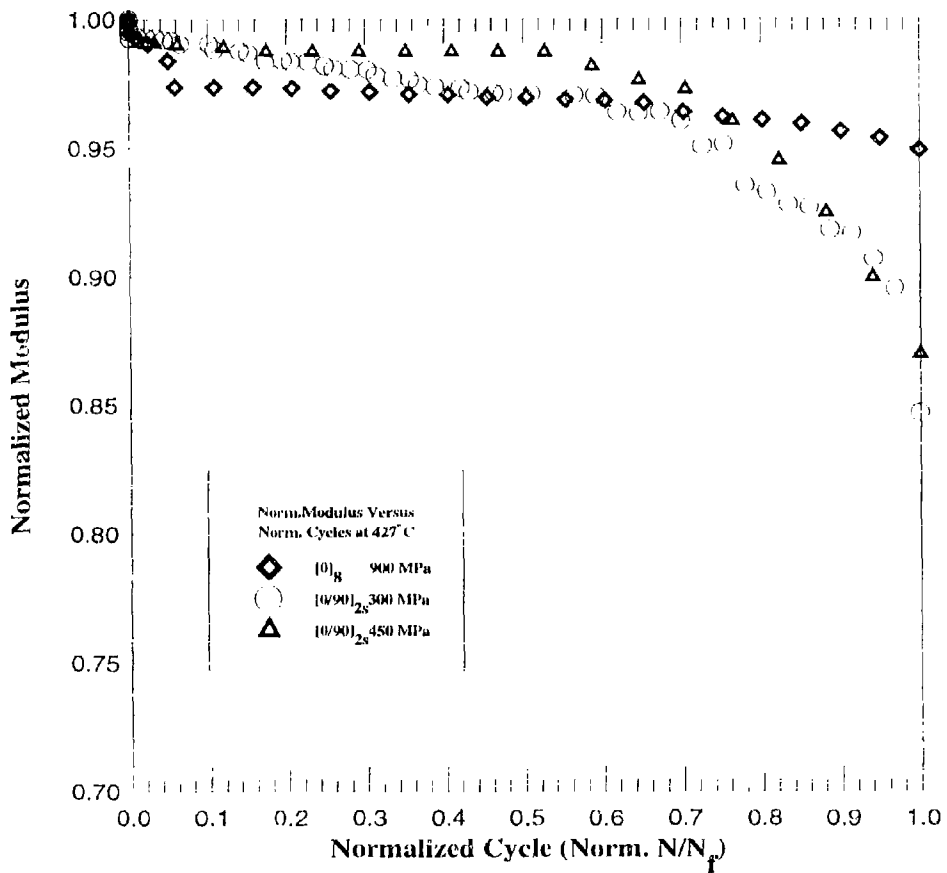
Figure 29. Normalized Modulus *vs* Normalized Cycles for $[0]_8$ & $[0/90]_{2s}$ Laminates
Fatigue Tests at 427°C, R=0.05, f=10 Hz(5Hz), σ_{max}=900, 450, 300 MPa
Conditions

The normalized residual strength vs normalized cycles is shown in Figure 30. The same general trend is observed in all tests as the residual strength drops rapidly near the end of the fatigue life. Also, a scatter in the specimen fatigue life of approximately a factor of two is observed. The comparisons of unidirectional, $[0]_8$, and cross-ply, $[0/90]_{2s}$ laminate tests including static, fatigue, and residual strength results are shown in Table 7.
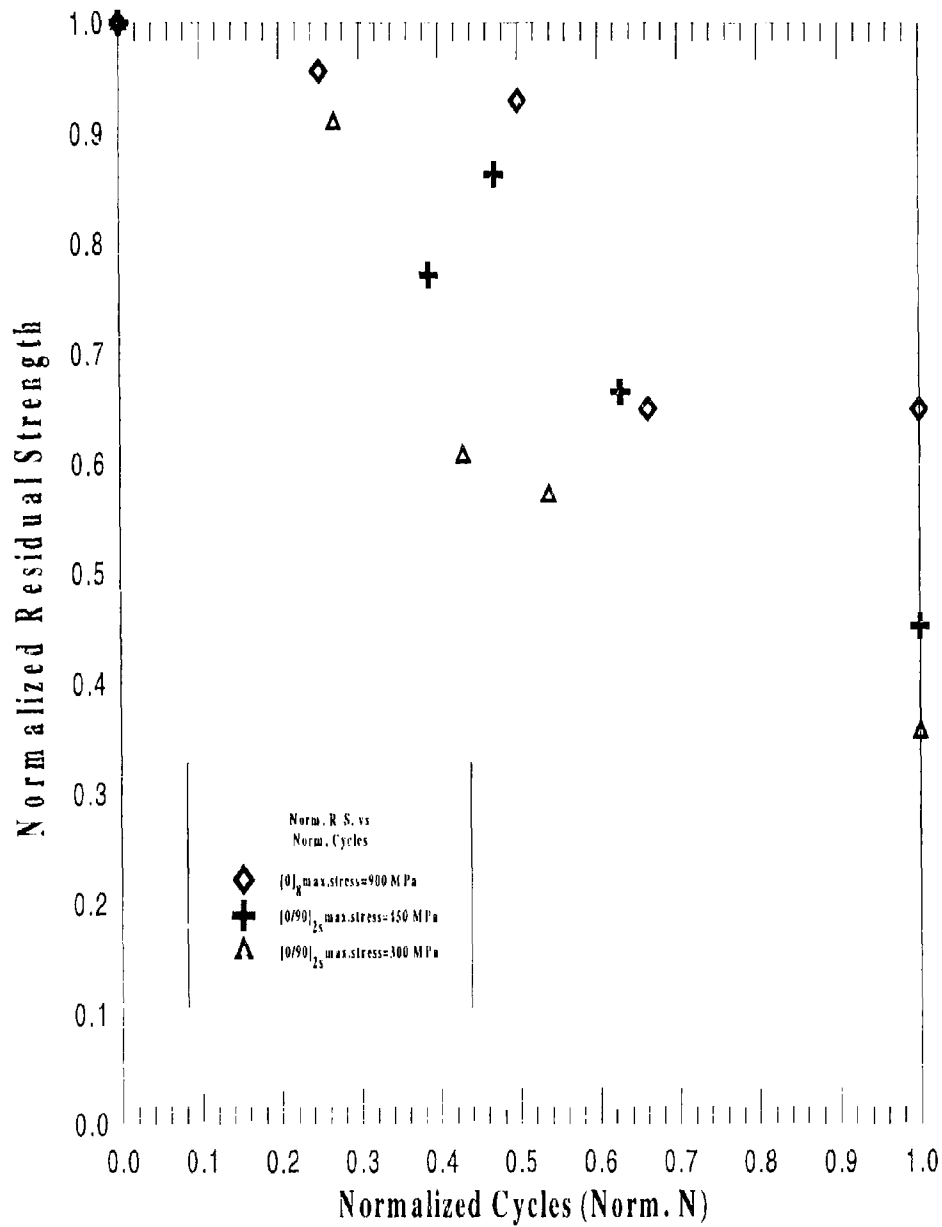
Figure 30. Normalized Residual Strength *vs* Normalized Cycles for [0]₈, & [0/90]₂ₛ Laminates at 427°C, R=0.05, f=10 Hz(5Hz), σ_{max}=900, 450, 300 MPa

45

Table 7. The Results of Static, Fatigue, Residual Strength Tests of $[0]_8$ & $[0/90]_{2s}$ at 427°C

Specimen Type	N	σ_{max} (MPa)	$\Delta \varepsilon_{max}$ (%)	$\Delta \varepsilon_{min}$ (%)	ΔE (GPa)	R.S. (MPa)	σ_{ult} (MPa)
$[0]_8$	7,645	900	0.002	0.0018	2.59	1324.5	(a)
"	15,284	"	0.014	0.0148	3.61	1287.0	"
"	20,004	"	0.0453	0.0462	13.75	900.0	"
"	20,224	"	0.1085	0.1182	8.51	900.0	"
"	*	-----					1,385.7
$[0/90]_{2s}$	6,598	450	0.049	0.0337	0.89	768.14	(b)
"	8,004	"	0.0205	0.0482	0.92	859.2	"
"	10,692	"	0.0298	0.0718	10.02	662.64	"
"	17,023	"	0.1014	0.0984	16.02	450.00	"
"	**	-----					995.86
"	50,010	300	0.0706	0.0495	5.13	767.17	(c)
"	80,010	"	0.0809	0.0509	11.4	511.62	"
"	100,010	"	0.0838	0.0610	19.27	481.20	"
"	186.000	"	0.1034	0.1041	28.54	300.00	"
"	***	-----					843.79

* Monotonic Test for Unidirectional $[0]_8$ Laminate with a Stress Rate of 15MPa/s
** & *** Monotonic Test for Cross-Ply $[0/90]_{2s}$ Laminates with a Stress Rate of 15MPa/s
The Applied Frequencies for (a) & (b), and (c) were 10Hz, 10Hz, and 5Hz, Respectively.

4.4. Microscopic Comparison

The typical distribution of the fibers within the metal matrix composite are shown in figure 31. The fiber volume fraction was approximately 0.35.
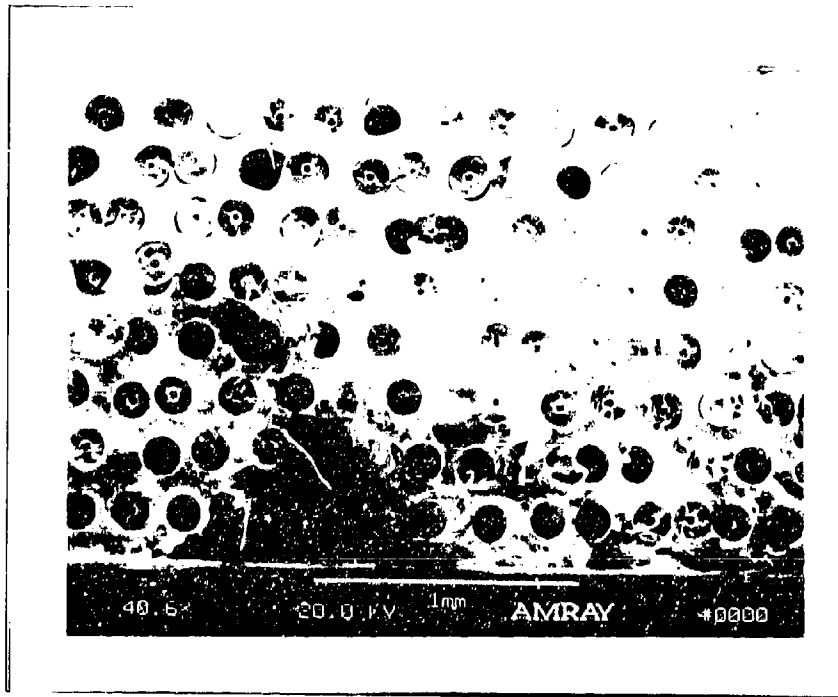
Figure 31. Fiber Distribution within the Laminate

4.4.1 Unidirectional, [0]₈, Laminate

Fracture analysis indicated interface debonding between fiber and the matrix during the tensile testing as the matrix exhibited plastic "necking" between the fibers as shown in Figure 32. Also, it is found that the degradation or the fracture of the fiber coating layer occurred during fatigue.

47
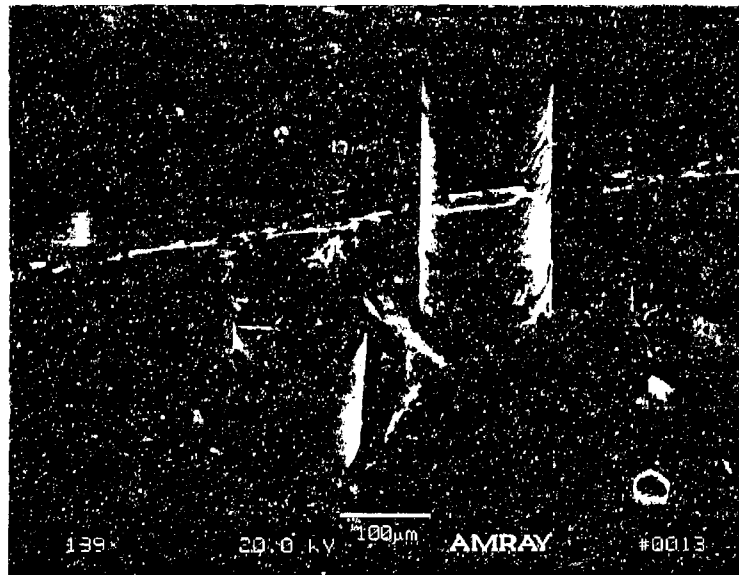
Figure 82 Matrix Plastic Necking between Fibers

Figure 83 Crack Initiation & Propagation from Interface of Fiber Matrix

Under the scanning electron microscope (SEM) observations, Figure 33 displays that cracks initiated from the fiber-matrix interface and propagated through the matrix.

During the tensile testing, a crack could initiate from the debonded fiber-matrix interface and extend to the debonded interface of the neighboring fiber. The micro-structural characteristics were evaluated near the fracture surface under SEM. Some cracks were observed along the longitudinal direction of the fiber. In Figure 34, the debonding between fiber and matrix was clearly observed. A crack which appeared to initiate from the debonding fiber-matrix interface of one fiber, extended to the debonded interface of the neighboring fiber. The crack propagated through the matrix as well as interface. Hence, interface debonding, matrix cracking, and fiber cracking contributed to the fracture process of tensile behavior.

Figure 34. Interface Debonding between Fiber-Matrix

4.4.1.1 Fiber Dominated Failure Mode

The progression of deformation and damage for the fiber-dominated failure mode was plastic deformation of the matrix, creep deformation of the matrix, and fracture of fibers which resulted in the failure of specimens. Figure 35 showed a typical fracture surface of a specimen that exhibited a fiber-dominated failure mode. Most of the fibers had pulled out of the matrix. The dimple patterns in the matrix represented the coalescence of microvoids, which was characteristic of a ductile fracture. This type of fracture surface was typical of the static tensile specimens and the low life fraction residual strength tests.

Figure 35. Fracture Surface Dominated by Fiber Failure Mode

4.4.1.2 Matrix Dominated Failure Mode

Figure 36 shows the first layer of fibers from the surface of the specimen. Several matrix cracks were observed. In addition to matrix cracking, there was also the debonding of the fiber-matrix interface. This phenomena explained the reduction in stiffness during the fatigue tests.

Figure 36. Fracture Surface Dominated by Matrix Failure Mode

4.4.2 Cross-Ply, $[0/90]_{2s}$, Laminate

During the fatigue of the cross-ply specimens, three stages of behavior were observed (as could be seen in Fig. 37). Strain in the stage I rapidly increased within the first few cycles due to plastic deformation. In the stage II, the strain increased steadily with fatigue cycles indicating a fatigue crack started to initiate and propagate. In stage III, the strain increased rapidly until composite failure, indicating the matrix crack was near its critical length and/or fiber failure was occurring. Also, due to the transverse plies in the cross-ply, the fatigue cracks in the unidirectional specimen were more difficult to initiate than in the cross-ply.
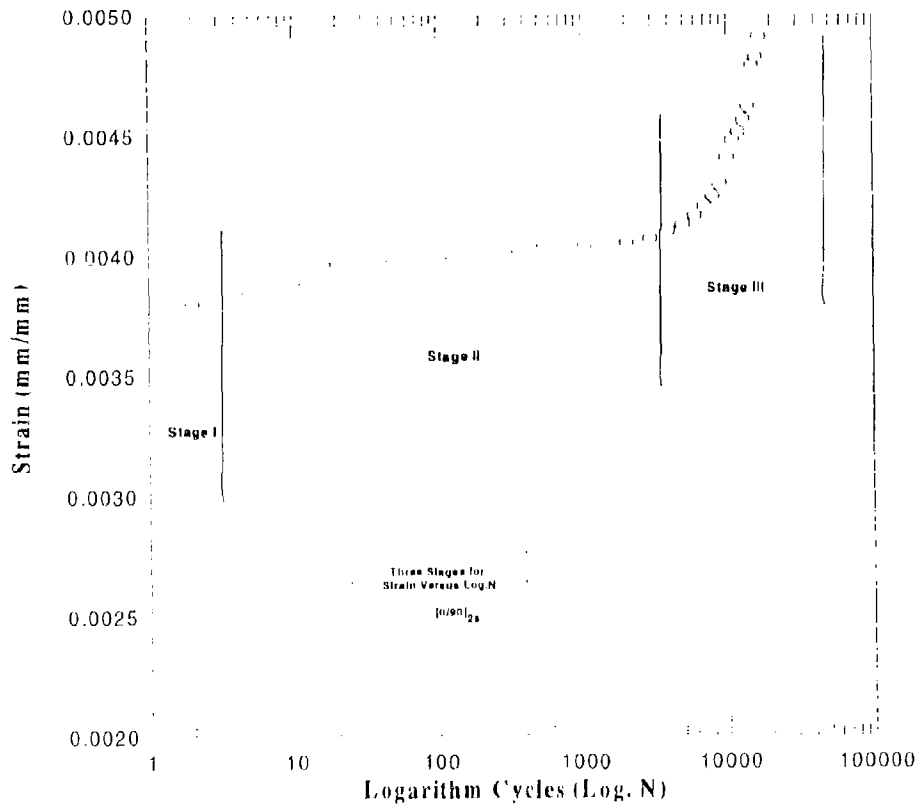
Figure 37. Three Stages for the Strain Cycles Response under Fatigue Test

The first damage mode that normally formed was matrix cracking along the transverse fiber directions. These cracks generally formed through the ply thickness and across the width of the specimen, and continued nucleating until a stable regular array of cracks typical of the laminate had formed.

4.4.2.1 σ_{max}=450 MPa

For the specimen cycled to 8,004 cycles, a crack appeared to have initiated from the transverse fiber located at the fiber-matrix interface and extended to the outer surface of the specimen. As fatigue cycling continued, the crack seemed to have propagated along the interface of the transverse plies and extended into the matrix of the 0^0 plies. Thus, matrix cracking and interface debonding seemed to be the dominant fracture mechanism during fatigue loading.

4.4.2.2 σ_{max}=300 MPa

The same type of fracture surface occurred at this stress as at a stress level of 450 MPa. At 80,000 cycles, a crack was observed to have initiated from the transverse fiber located inside of the specimen as demonstrated in Figure 38. These cracks seemed to have initiated from the transverse fiber on the basis of the previous discussion.

4.4.2.3 Comparison between σ_{max}=450 MPa and σ_{max}=300 MPa

Both at a stress level of 450 MPa and 300 MPa, each crack initiated from the transverse fiber, propagated to the surface, grew along the interface of the transverse fiber and the matrix, extended into the matrix and continued extending along the interface of neighboring fibers and finally penetrated into the 0° plies. Therefore, matrix cracking and interface debonding appeared to be the prime fatigue fracture mechanisms. The number of observed cracks increased with increasing applied cycles.
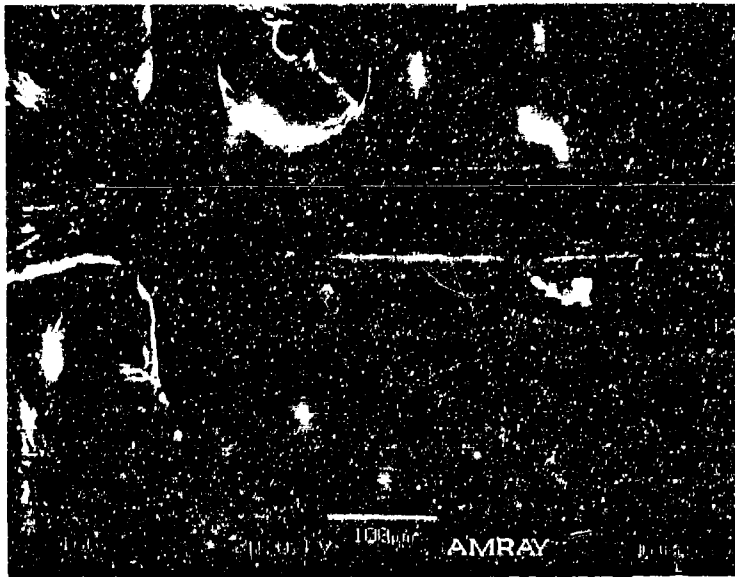
Figure 38. Crack Initiated from Transverse Fiber Direction

4.4.3 Observations of Etched & Polished Specimens

As previously discussed, the fractography of monotonic loading tests for unidirectional and cross-ply laminates near the fracture surface revealed that the failure was dominated by the strength of the fibers as shown in Figures 39 and 40. For the fatigue tests of the unidirectional laminates, fiber-matrix interface debonding was the source of crack initiation sites within the matrix. These matrix cracks propagated transversely from the longitudinal fiber direction. The cross-ply specimens displayed a similar trend except the damage initiated at the interface of the 90" plies and then propagated along the interfaces and through the matrix from fiber to fiber within the 90" plies.
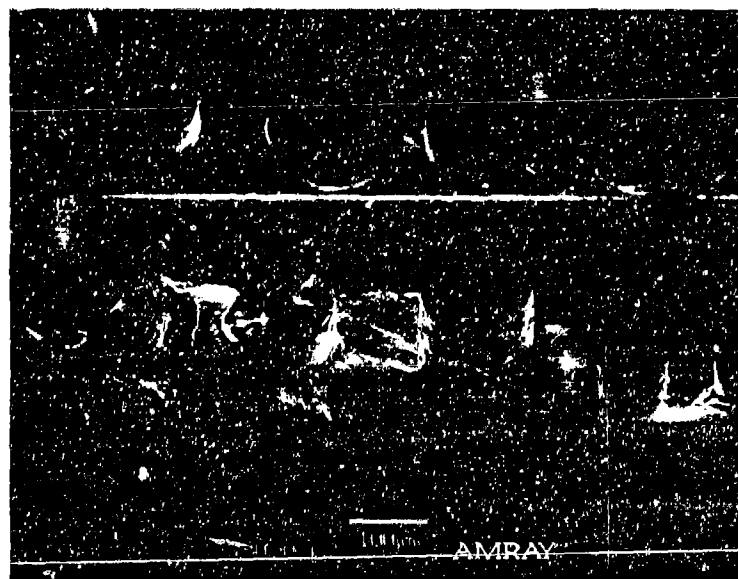
Figure 39. Fiber Dominated the Monotonic Load Failure
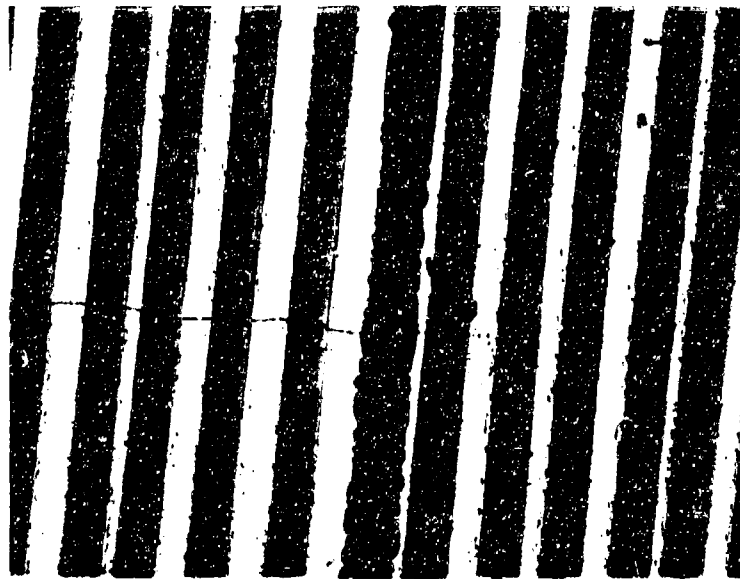
Figure 40. Cracks Propagated Transverse to the Loading Direction

4.4.3.1 For [0]$_8$ Laminate

The observations of etching and polishing specimen of the unidirectional laminate away from the fracture surface are shown in Figures 41 through 46. There was no crack or interface debonding for 25%, 50% of the fatigue life of the first fatigued specimen but at 75% there occurred some fiber-matrix interface debonding and matrix failure.
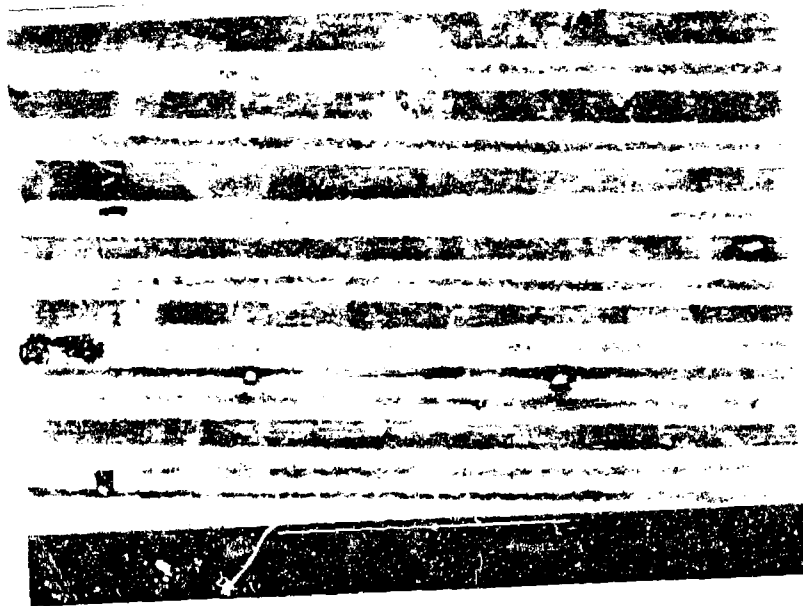
Figure 41. Etching Observation on 25 % N_f of $[0]_3$ Laminate, σ_{max}=900 MPa
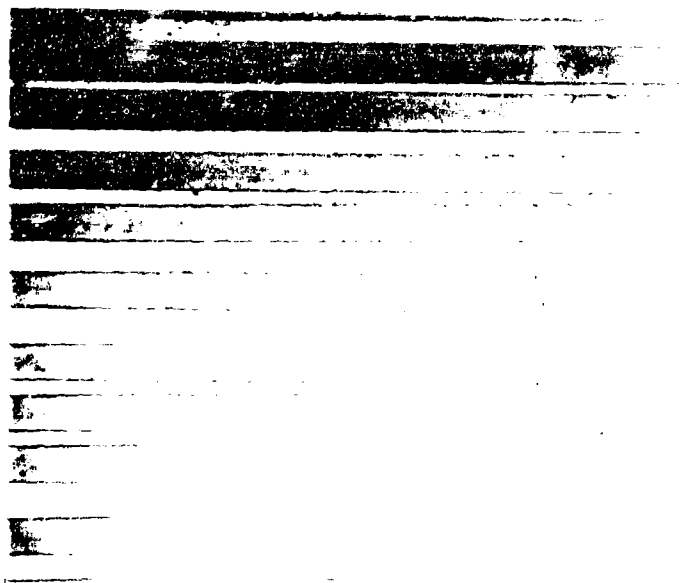
Figure 42. Polishing Observation on 25 % N_f of $[0]_8$ Laminate σ_{max}=900 MPa
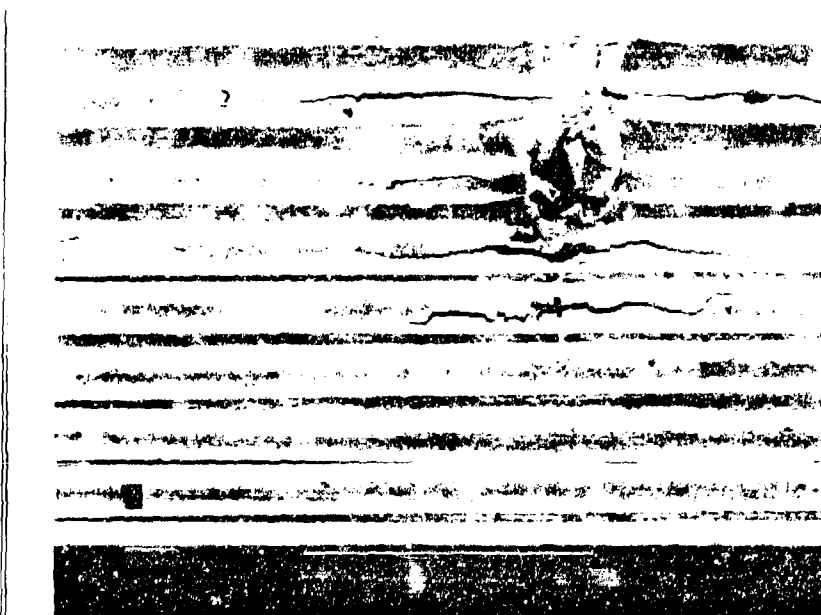
Figure 43. Etching Observation on 50 % N_f of $[0]_8$ Laminate, σ_{max}=900 MPa

Figure 44. Polishing Observation on 50 % N_f of $[0]_8$ Laminate, σ_{max}=900 MPa
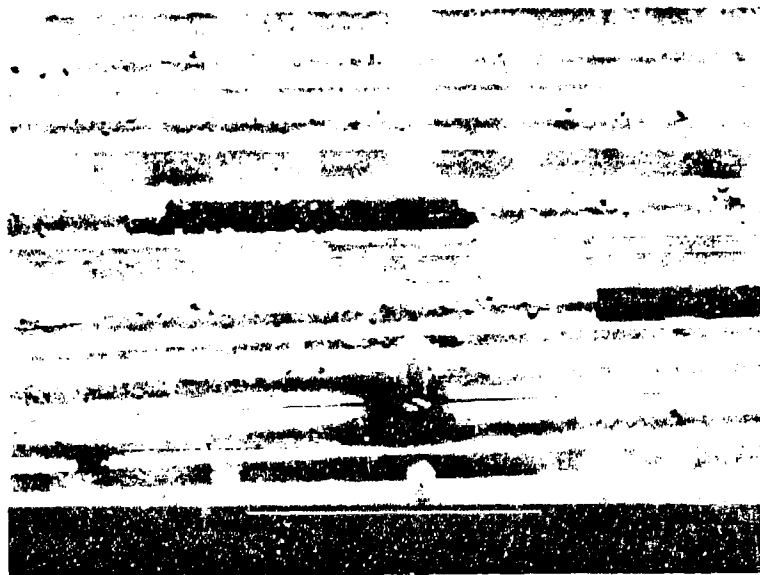
Figure 45. Etching Observation on 75 % N_f of $[0]_8$ Laminate, σ_{max}=900 MPa

Figure 46. Polishing Observation on 75 % N_f of $[0]_8$ Laminate, σ_{max}=900 MPa

4.4.3.2 For $[0/90]_{2s}$ Laminate

The same phenomenon as was observed in the unidirectional laminate occurred in the cross-ply. The matrix failed throughout the width of the specimen at near the end of fatigue life as shown in Figure 47. Before two-thirds of the fatigue life of the first fatigued specimen, the damage of these cross-ply lamina are the same regardless of the effect of the applied stress level, i.e., the applied stress, 450 N pa and 300 Mpa did not affect the mode of the fatigue failure. Further discussion of the damage modes and additional photographs are presented in chapter 5.

Figure 17 Polishing Observation on 100 % N_f of [0/90]s Laminate.
σ_{max} ~ 800 MPa

5. Discussion

5.1 Deformation Mechanisms

Fatigue life response can be divided into three distinct regions, see Figure 48 [21]. In the low cycle region (within 200 cycles) the applied stress level is slightly dependent upon cycling.
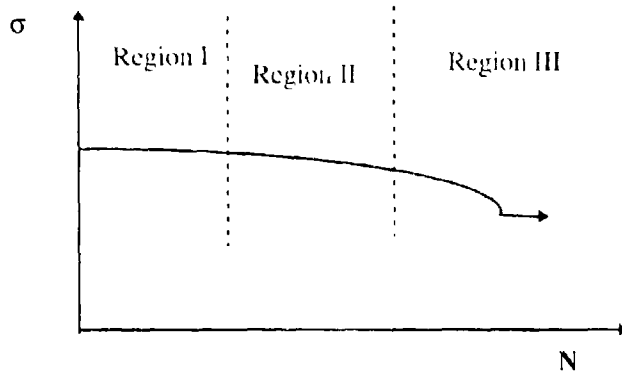
Figure 48. Three Regions Response for Fatigue

In the high stress/low cycle region ($> 10^5$), the strength is highly dependent on the fiber mean strength and strength distribution. In the second region (200 to 10^6 cycles), the logarithm of the applied stress decreases almost linearly with the number of cycles. Fatigue failure in this region occurs by the growth of matrix microcracks leading to preferential fiber failure. In the third region, the applied stress was below the microcrack initiation stress. For low fatigue strains, damage initiates in the matrix and the composite possesses a longer fatigue life than the matrix itself.

Fatigue damage consists of various combinations of matrix cracking, debonding, delamination, void growth, and fiber breakage, *etc*. As a result, fatigue cannot be defined in terms of a single failure mode. A common consequence of fatigue in composite is a reduction in stiffness which begins very early in the fatigue life (see Figures 10, 17, and 29).

Hence, it is possible to define fatigue failure in terms of stiffness reduction. However, for the present study only a slight reduction in stiffness was observed over the life (less than 10 %). Also, this quantity was difficult to measure at the required level of accuracy.

The test specimens were cut from a large, continuously reinforced plate and, consequently, contained cut fibers along the edges. These locations were potential stress concentration or crack initiation points. Metallography of the fatigued specimens revealed extensive matrix cracking throughout the entire cross section of the specimen as can be seen in Figure 49.

5.1.1 Plastic Deformation

The plastic deformation in the metal matrix renders the result that the overall stress response becomes a strong function of the applied loading path as well as the fiber orientation and distribution within the ductile matrix. The fiber volume fraction is approximately about 0.35 (see Fig. 31). When the unidirectionally reinforced composite is loaded in tension along the axis of the fibers, the load is carried primarily by the brittle elastic fibers and there is very little plastic deformation in the intervening ductile matrix.

Figure 49. Matrix Cracks Throughout the Width

After certain cycles, since the specimen was under high temperature, the titanium based matrix experienced creep and became unable to sustain the load, thereas, the load was distributed to the fibers. This caused an increased stress on the fibers and a greater mean strain on the composite.

5. 2 Macroscopic Observations

The present study depicted a traditional stress-strain response during cycling for a specimen whose dominant failure mode was matrix cracking. A non-linear stress-strain relationship was observed in the first few cycles. This was a result of plastic deformation of the matrix.

5.2.1 Macromechanical Response for $[0]_8$ Laminate

The modulus vs cycles (Fig. 10) curve depicts a drop in the modulus after approximately two-thirds of the fatigue life of the first fatigued specimen. The strain vs cycles (Fig. 12) curve also indicates composite damage near the end of the fatigue life due to the increasing strain. Thus, these plots suggest the majority of the damage occurs near the end of the fatigue life.

5.2.2 Macromechanical Response for $[0/90]_{2s}$ Laminate

From Figures 17 and 29, the modulus did not drop much with the increasing cycles until approximately two-thirds of the total fatigue life. The modulus decrease was accompanied by a strain increase which represented that the damage had been formed within the laminate. Also, the residual strength results demonstrated significant scatter in the data with a rapid drop in strength near the end of the fatigue life. These trends indicate the existance of a critical point in the matrix crack propagation where the strength decreases rapidly with cycles. Also, the data scatter may point to the statistical variation in fiber strength along the matrix crack.

5. 3 Microscopic Responses

5.3.1 Micromechanical Response for [0]$_8$ Laminate

Figure 50 shows a typical fracture surface of a specimen that presented a ductile-matrix failure mode. Most of the fibers had been pulled out of the matrix. This represents the tensile overload failure. All fractured specimens possessed an area of the surface exhibiting these characteristics. The only difference was the percent of the surface that could be classified as overload region. The specimens with more fatigue life possessed a smaller ductile overload surface. The percentage of the fracture area dominated by fatigue or by overload for individual unidirectional tested specimen are shown in Figures 51, 52, and 53, and Table 8.
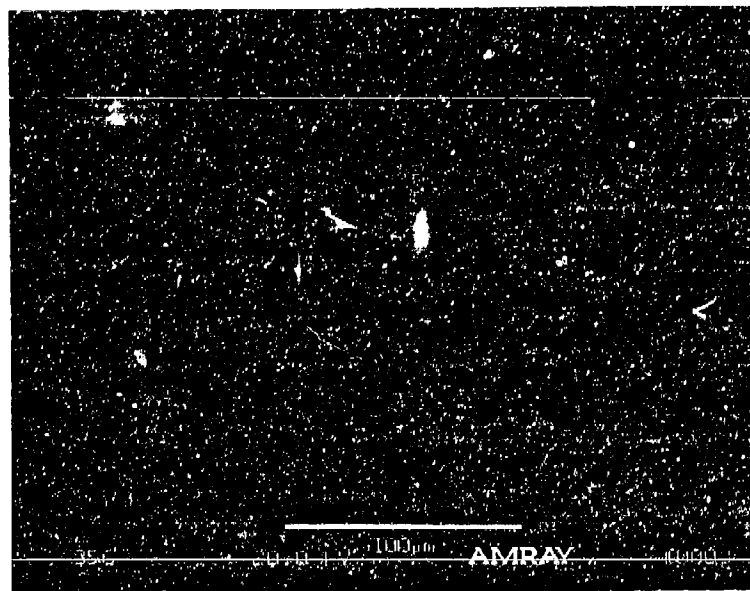
Figure 50. Fracture Failure Dominated by Matrix
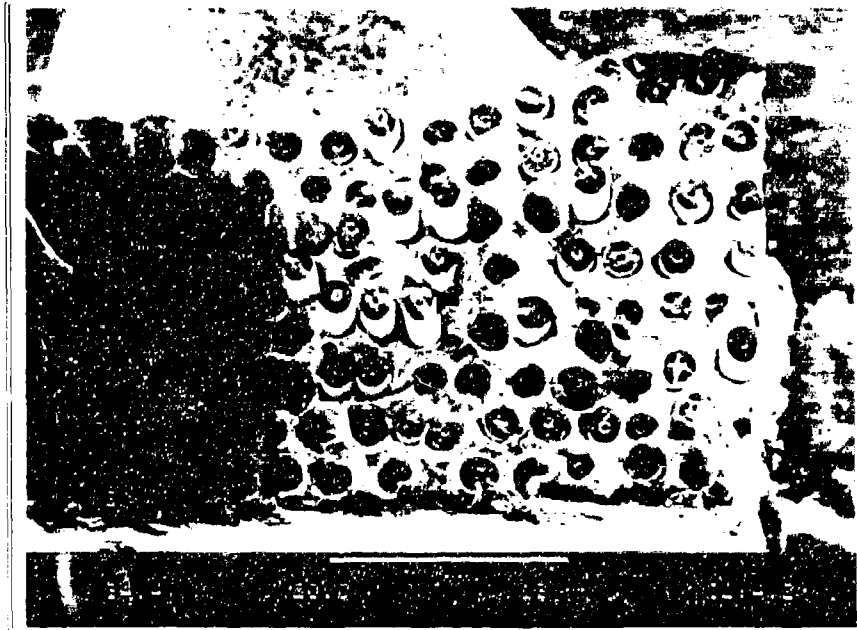
Figure 51. 25% N_f of the Unidirectional Laminate, $\sigma_{max} = 900$ MPa
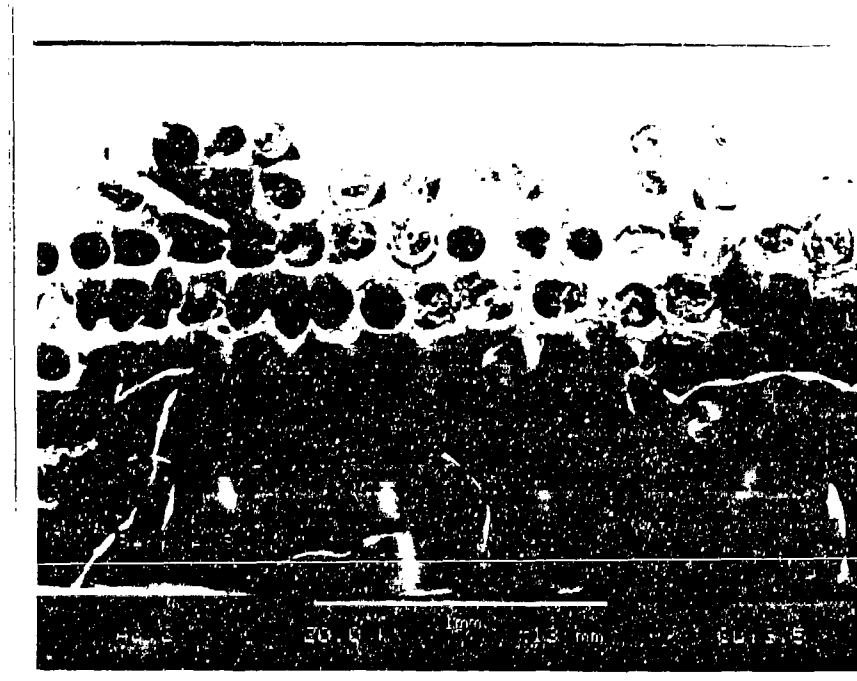
Figure 52. 50% N_f of the Unidirectional Laminate, $\sigma_{max} = 900$ MPa
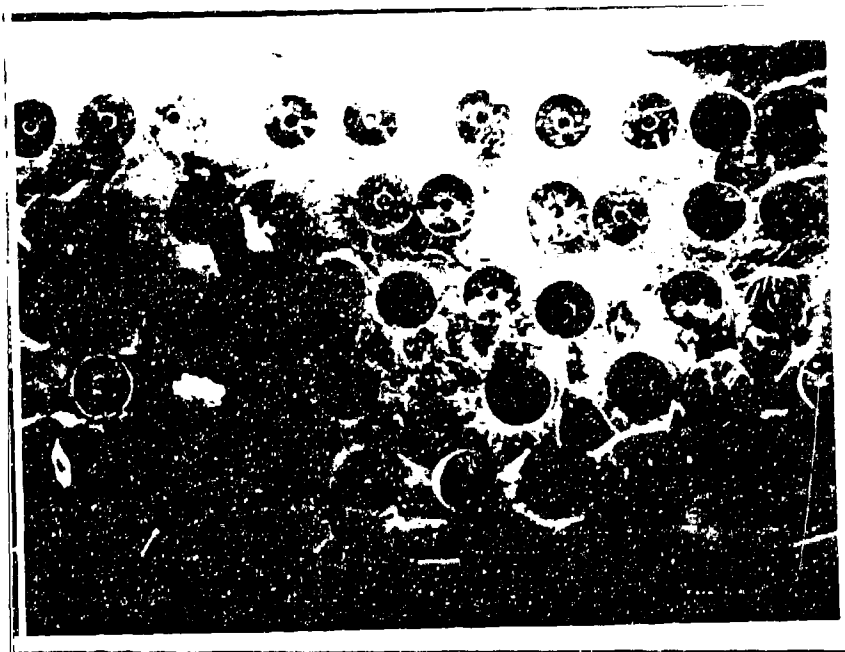
Figure 53. 75% N_f of the Unidirectional Laminate, σ_{max}=900 MPa

Table 8. The Percentage (%) of Failure Dominated by Fatigue or Overload for $[0]_8$ Laminate

Specimen Type	Maximum Stress (MPa)	Applied Cycle	Fatigue (%)	Overload (%)
$[0]_8$	900	7,645	70	30
"	"	15,284	75	25
'	"	20,244	85	15

The matrix, between failed fibers, had some dimple patterns as can be seen in Figure 54. This indicated that the matrix experienced ductile necking between broken fibers during the final fracture.
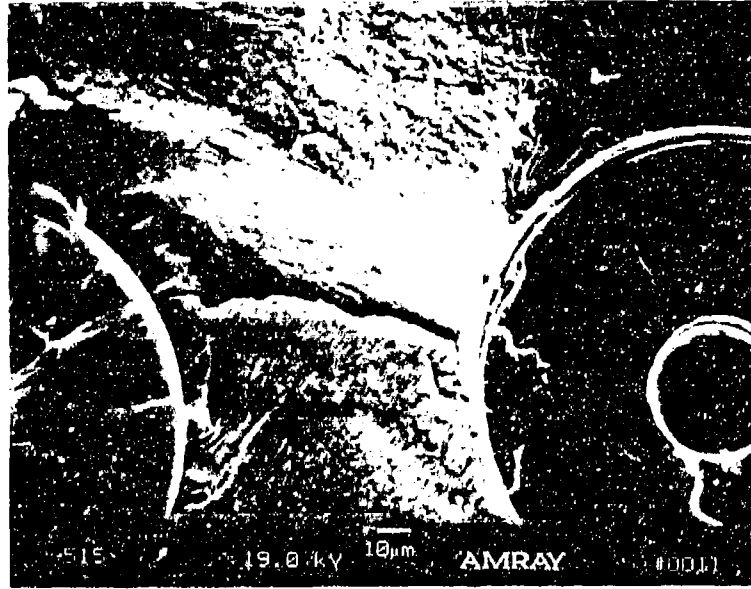
Figure 54. Matrix Failure between Fibers

5.3.2 Micromechanical Observations for [0/90]₂ₛ Laminate

The primary fatigue damage initiation mechanism in all the tests was the transverse cracks originating at the interface of 90° fibers and then propagating outward from 90° fibers. The transverse matrix cracks originated at the interface in 90° fiber, propagated toward 0° fibers and deflected in 0° fiber direction due to the weaker interface. The microscopic observations showed a two region failure behavior for specimens with a matrix dominated failure mode. This was observed in the fracture surface which consisted of two distinct areas. A fatigue crack growth region was observed which possessed fatigue striations and a relatively even surface along crystalographic planes of the matrix. The other area consisted of ductile matrix failure through void coalesence. Both regions demonstrated fiber pullout. The percentage of the fracture area dominated

by fatigue or by overload for each cross-ply specimen are shown in Figures 55 through 60, and Table 9.
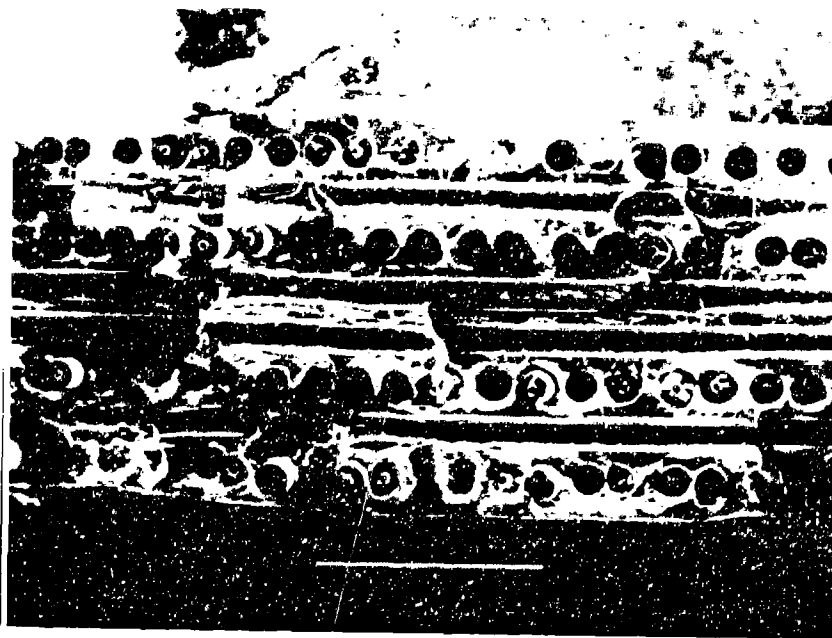
Figure 55. 25% N_f of the Cross-Ply Laminate. σ_{max}=450 MPa
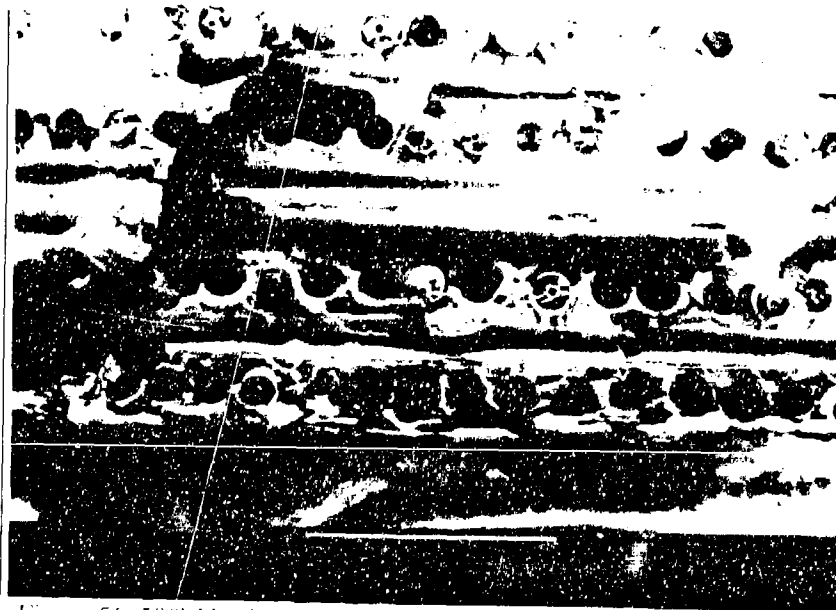
Figure 56. 50% N_f of the Cross-Ply Laminate, σ_{max}=450 MPa
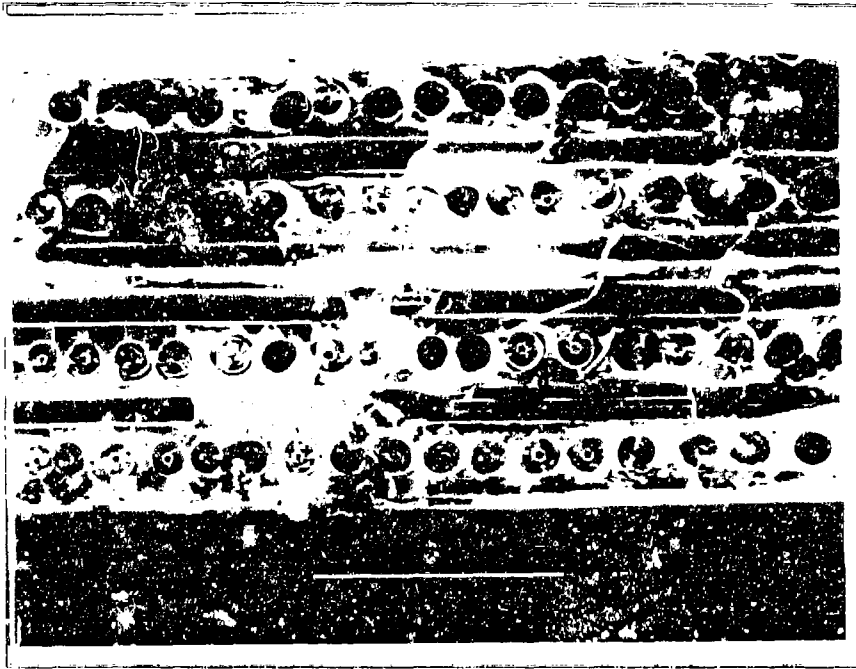
Figure 57. 75% N_f of the Cross Ply Laminate, σ_{max} = 450 MPa
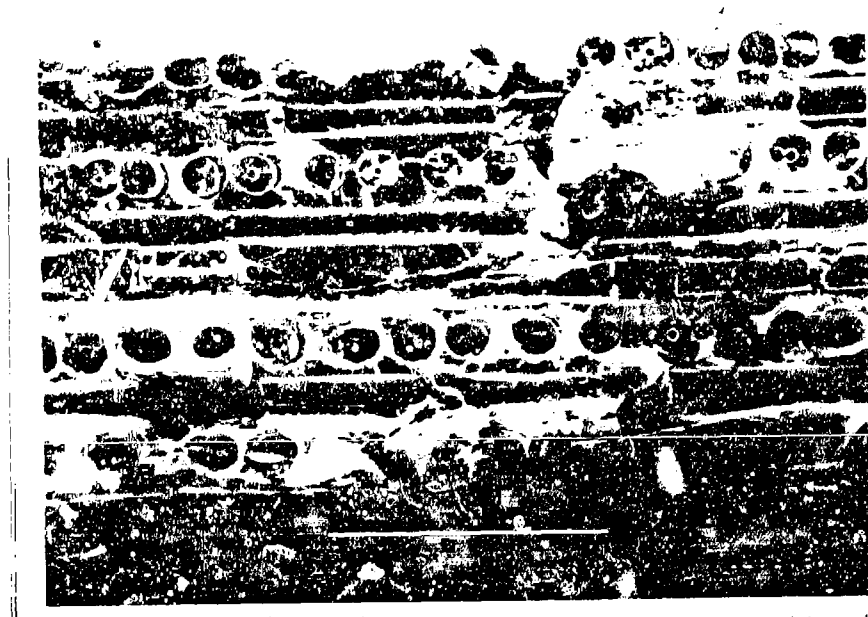
Figure 58. 25% N_f of the Cross Ply Laminate, σ_{max} = 400 MPa
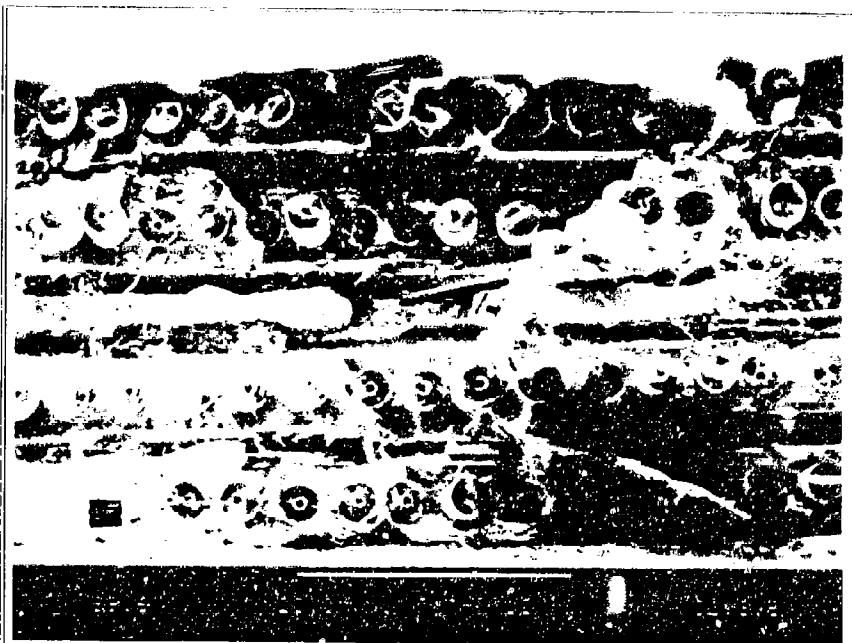
Figure 59. 50% N_f of the Cross Ply Laminate, σ_{max} = 300 MPa

Figure 60. 75% N_f of the Cross Ply Laminate, σ_{max} = 300 MPa

Table 9. The Percentage (%) of Failure Dominated by Fatigue or Overload for [0/90]₂ₛ Laminate

Specimen Type	Maximum Stress (MPa)	Applied Cycle	Fatigue (%)	Overload (%)
[0/90]₂ₛ	450	6,598	~70	~30
"	"	8,004	~60	~40
"	"	10,692	~75	~25
"	300	50,010	~75	~25
"	"	80,010	~80	~20
"	"	100,010	~85	~15

There were three types of fatigue damage mechanism... (see Figure 61) which were fiber breakage, matrix crack, and fiber-matrix debonding. Damage was defined by the creation of new free surfaces from fiber and matrix crack growth. Fiber and matrix cracks could cause debonding between the fiber and matrix which prevented the fibers from transferring any load to the matrix, and debonding might also occur from low interface strength caused by poor materials processing. Extreme necking around fibers showed a great deal of debonding.
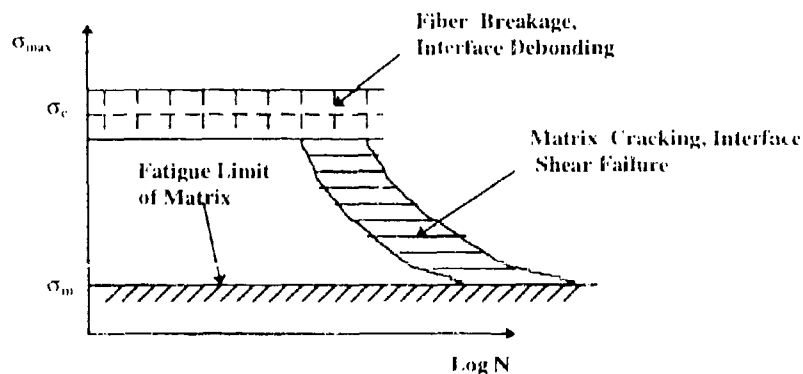
Figure 61. Three Fatigue failure modes for [0]₈ under Load Parallel to Fibers

Although the present study examined only a single load level (900 MPa) for the unidirectional layup, the same failure mechanisms were observed as in the fatigue life map (Fig. 61). The specimens loaded to a small fraction of the fatigue life and then loaded to failure for residual strength testing experienced ductile matrix failure and fiber overload. Specimens fatigued through a significant portion of the life demonstrated more matrix cracking.

The microstructures of several polished composite samples were investigated. This observation indicated that during the fracture processing, interface debonding between SiC, coating layer, and carbon core occurred. Also, matrix plasticity was evident from slip bands oriented at approximately 45° from the fiber axis.

If the fracture initiates in the matrix and the crack was allowed to grow along the fiber matrix interface without a fiber fracture, the reduction in stiffness was very small. This was apparent because matrix cracks were observed in the residual strength tests yet there was little reduction in stiffness. If the fracture initiated and progressed along the fiber matrix interface, there was almost no reduction in the longitudinal stiffness. Following a fiber fracture, the crack might grow either in the matrix or along the fiber matrix interface. Debonding along the fiber matrix could be caused by shear-stress or the stress in the transverse direction.

5.4 Data Analysis

Residual Strength Prediction Model

It is desired to develop a single equation with normalized parameters which can relate the residual strength of the given material to the applied load and the number of cycles. The following power law relation is proposed [22]:

$$1 - f = [1 - p] (N/N_f)^\lambda \qquad \text{(Eq. 1)}$$

where $f = \sigma_r / \sigma_{ult}$; σ_r : residual strength after applied fatigue cycles

σ_{ult} : ultimate strength of MMC

$p = \sigma_a / \sigma_{ult}$; σ_a : applied stress

N/N_f : life fraction

λ : parameter

where λ is a parameter introduced to accommodate the nonlinearity in the residual strength curve and is a parameter which is associated with nonlinearity of degradation in composite laminates.

Figure 62 shows a least squares best fit for the three sets of test conditions of the present study. The values of the f_r, p, λ based on the experimental data and λ is calculated by Eq. 2. as shown in Table 8.

$$\lambda = \frac{\sum_{i=1}^{n} [Log(1 - f) - Log(1 - p)][Log(\frac{N_i}{N_f})]}{\sum_{i=1}^{n} [Log(\frac{N_i}{N_f})]^2} \qquad \text{(Eq.2)}$$

75
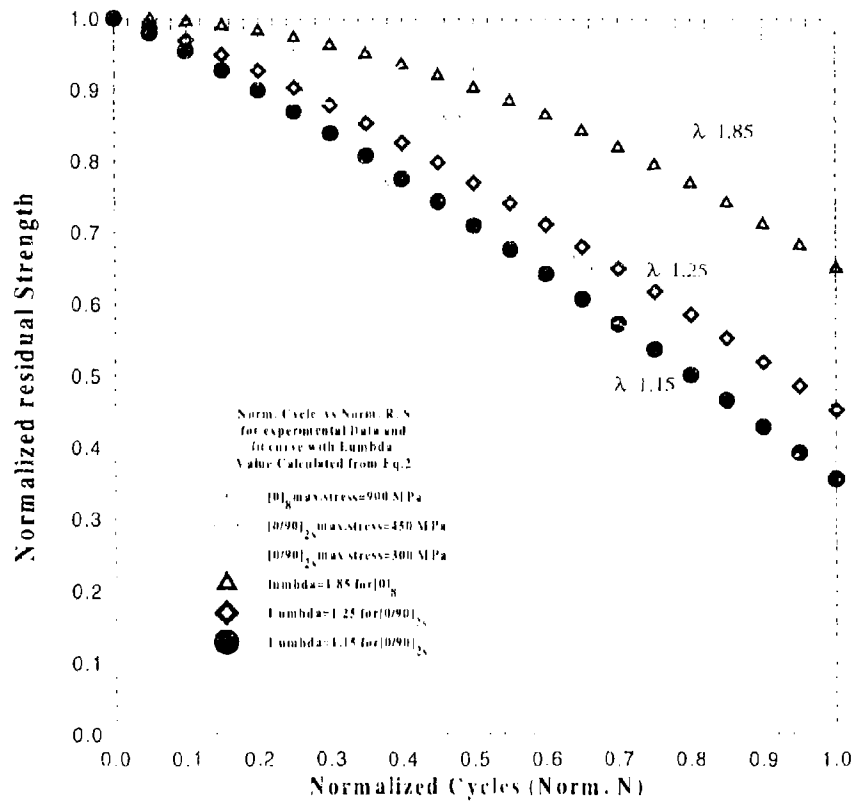
Figure 62. The Fit λ Values for [0]₈ & [0/90]₃ₛ Calculated by Eq.2

Table 10. The Values of Material Parameter (λ) Calculated by Eq.2

| [0]₈ =900 MPa | | [0/90]₃ₛ =450 MPa | | [0/90]₃ₛ =300 MPa | |
| λ=1.85 | | λ=1.25 | | λ=1.15 | |
N_i/N_f	$f=\sigma_r/\sigma_{ult}$	N_i/N_f	$f=\sigma_r/\sigma_{ult}$	N_i/N_f	$f=\sigma_r/\sigma_{ult}$
0.2502	0.9558	0.3876	0.7713	0.2689	0.9092
0.5001	0.9288	0.4702	0.8628	0.4302	0.6063
0.6624	0.6495	0.6281	0.6654	0.5377	0.5703
1.0000	0.6495	1.0000	0.4519	1.0000	0.3555

6. Conclusions

The present study investigated the residual strength of the unidirectional and cross-ply SCS-6/Ti-15-3 composite layups at elevated temperature (427°C). The specimens were fatigued to various fractions of the fatigue life of the first fatigued specimen and then loaded monotonically to failure. The purpose was to determine the effects of given levels of fatigue damage on the composite's strength.

All tests were conducted under load controlled tension-tension mode at 427 °C. The unidirectional specimens were cycled to a 900 MPa maximum stress at a frequency of 10 Hz, while the cross ply specimens were tested at both 300 MPa and 450 MPa at 5 Hz and 10 Hz, respectively. The residual strength results for the all three cases exhibited similar trends in that the residual strength drop with cycles was small until near the end of the fatigue life. Thus, the material exhibited a critical or catastrophic failure behavior as the presence of damage must reach a critical level before it has much effect on the composite. Beyond this point, the damage progressed rapidly to composite failure.

Based on a combination of fatigue tests, monotonic test, macroscopic observations, and fracture surface analysis. The following conclusion can be made from this investigation:.

1. The failure mode for the monotonic tests was dominated by the strength of the fibers for both longitudinal and cross-ply laminates. Also, the inelastic deformation of the composite was found to be dominated by matrix plasticity.

2. For the unidirectional laminate fatigue tests, debonding of the fiber matrix interface occurred first. This produced damage initiation sites. These damage sites were both on the

surface and internal. Matrix cracks from these damage sites proceeded to propagate transverse or perpendicularly from the load and fiber directions. Once these cracks reached the critical length, the composite failed. The cross-ply specimens displayed a similar trend except the damage initiated at the interface of the 90° fibers. These cracks propagated along the interfaces and through the matrix from fiber to fiber within the 90° plies. The matrix crack then penetrated to 0° plies and eventually grew to a critical length.

3. Both the unidirectional and cross-ply specimens demonstrated only a small dependence of the residual strength with cycles until near the end of the fatigue life. This residual strength behavior coupled with the observation of little or no fiber cracks away from the fracture surface suggests that the critical matrix crack was completely bridged by the fibers for most of the fatigue life.

Bibliography

1. Lerch, B. A., Gabb, T. P., MacKay, R. A., " Heat Treatment Study of the SiC/Ti-15-3 Composite System," *NASA TP-2970*, January, 1990.

2. Johnson, W. S., Lubowinski, S. J., Highsmith, A. L., " SCS-6/Ti-15-3 Metal Matrix Composite at Room Temperature," *NASA TM-1014*, April, 1988.

3. Gabb, T. P., Gayda, J., MacKay, R. A., " Isothermal and Nonisothermal Behavior of a Metal Matrix Composite," *Journal of Composite Material*, Vol. 24, June, 1990.

4. Castelli, M. G., Ellis, J. R., Bartolotta, P. A., "Thermomechanical Testing Techniques for High Temperature Composite: TMF Behavior of SCS-6/Ti-15-3," Sverdrup Technical Publication, 1990.

5. Lerch, B. A., Saltsman, J. F., " Tensile Deformation and Damage in SiC Reinforced Ti-15V-3Cr-3Al-3Sn," *NASA TM-103620*, NASA, Lewis Research Center, 1990.

6. Pollock, W. D., Johnson, W. S., " Characteristization of Unnotched SCS-6/Ti-15-3 Metal Matrix Composites at 650°C, " *NASP TM 102699*, September, 1990.

7. Mall, S., Portner, B., " Investigation of Fatigue Damage Mechanism in a Metal Matrix Composite under Elevated Temperature, " *MS Thesis, AFIT/GAE/ENY/90D*, School of Engineering, Air Force Institute of Technology, Wright-Patterson AFB, OH., December, 1990.

8. Majumdar, B. S., Newaz, G. M., " A Comparison of Mechanical Response of MMC at Room and Elevated Temperature," *Composite Science and Technology.*, 50, 1994.

9. Majumdar, B. S., Golam, M., Newaz, G. M., "Inelastic Deformation of Metal Matrix Composite, Plasticity and Damage Mechanisms, " Part I and II, *NASA Contractor Report 189096*, December, 1992.

10. Naik, R. A., Johnson, W. S.,"Observations of Fatigue Crack Initiation and Damage Growth in Notched Titanium Matrix Composite," *Paper Presented at ASTM Third Symposium on Composite Composite Material*: Fatigue and Fracture, Orlando, FL., November, 1989

11. Boyum, E. E.," Investigation of Tension Compression Fatigue of a Cross Ply [0/90], Metal Matrix Composite at Room and Elevated Temperature," *MS Thesis, AFIT/GAE/ENY/93D*, School of Engineering, Air Force Institute of

Technology, Wright-Patterson AFB, OH., December, 1993.

12. Highsmith, A. L., Reifsnider, K. L., " Stiffness Reduction mechanisms in Composite Laminates, " *Damage in Composite Materials, ASTM STP 775*, American Society for Testing and Materials, 1982.

13. Hahn, H. T., Tsai, S. W., " On the Behavior of Composite Laminates After Initial Failure, " *Journal of Composite Materials*, 8, 1974.

14. Gottesman, T., Hashin, Z., Brull, M. A., " Elastic Moduli of Cracked Fiber Composite, " *Advances in Composite Materials*, Vol. 1, Bunsell, A. R. *et al.*, eds., Pergamon Press, Oxford, 1980.

15. Gayda, J., Gabb, T. P., Freed, A. D., *NASA TM 101984*, Cleveland, OH : NASA Lewis Research Center, 1989.

16. Mall, S., Ermer, P. G.," Thermal Fatigue Behavior of a Unidirectional SCS-6/Ti-15-3 Metal Matrix Composite, " *Journal of Composite Materials*, 25, 1991.

17. Khan, T., Stohr, J. F., Bibring, H., " Supperalloys (Tien, J. K., Wlodek, S. T., Morrow, H. *et al.* eds), " Warrendale PA: *ASM*, 1980.

18. McLean, M., In" Fatigue and Creep of Composite Materials (Lilholt, H., Talreja, R. eds)," Roskilde, Denmark: Riso National Library, 1982a.

19. Das, G., " Process on Fundamental Relationships between Microstructures and Mechanical Properties of Metal Matrix Composite dungor, M. N., Liaw, P. K., eds., *TMS* Warrendale, PA., 1990.

20. Kraabel, D. L.," Investigation of Tension-Compression Fatigue Behavior of a Unidirectional Metal Matrix Composite at Elevated Temperature, " *MS Thesis, AFIT/GAE/ENY/94D*, School of Engineering, Air Force Institute of Technology, Wright-Patterson AFB, OH., December, 1994.

21. Dharan, C. K. H., " Fatigue Failure Mechanisms in a Unidirectionally Reinforced Composite Materials, " *Fatigue of Composite Materials, ASTM STP 569*, American Society for Testing and Materials, 1975.

22. Reifsnider, K. L., Stinchcomb, W. W., " A Critical Element Model of the Residual Strength and Life of Fatigue Loaded Composite Coupons, " *Composite Materials: Fatigue and Fracture ASTM, STP 907*, Hahn, H. T., Ed., American Society for Testing and Materials, 1986.

80

Vita

Major Sen-Tzer Chiou ████████████████████████████████

████ He graduated from Kaohsiung High School in 1980 and entered Chung Cheng Institute of Technology. In 1986, he graduated with a Bachelor of Material Science & Engineering in the Department of Mechanical Engineering and was commissioned as a first lieutenant in the Republic of China Army in Taiwan. His first tour of duty was in the 202th Arsenal at Combined Forces Service in Taipei. There he served at the heat treatment plant and guntube manufacturing division. Before being assigned to AFIT, he stayed in Defense Language Institute (DLI), Lackland, AFB, TX for 8 weeks' English Training and entered the Graduate School of Engineering of the Air Force Institute of Technology in May of 1994.

████████████████████████████████

94

REPORT DOCUMENTATION PAGE

Public reporting burden for this collection of information is estimated to average 1 hour per response, including the time for reviewing instructions, searching existing data sources, gathering and maintaining the data needed, and completing and reviewing the collection of information. Send comments regarding this burden estimate or any other aspect of this collection of information, including suggestions for reducing this burden to Washington Headquarters Services, Directorate for Information Operations and Reports, 1215 Jefferson Davis Highway, Suite 1204, Arlington, VA 22202-4302, and to the Office of Management and Budget, Paperwork Reduction Project (0704-0188) Washington, DC 20503

1. AGENCY USE ONLY (Leave blank)	2. REPORT DATE June 1996	3. REPORT TYPE AND DATES COVERED Master Thesis

4. TITLE AND SUBTITLE
Residual Strength After Fatigue of Unidirectional and Cross-Ply Metal Matrix Composites at Elevated Temperature

5. FUNDING NUMBERS

6. AUTHOR(S)
Sen-Tzer Chiou, Maj, R. O. C. ARMY

7. PERFORMING ORGANIZATION NAME(S) AND ADDRESS(ES)
Air Force Institute of Technology, WPAFB OH 45433-7765

8. PERFORMING ORGANIZATION REPORT NUMBER

9. SPONSORING/MONITORING AGENCY NAME(S) AND ADDRESS(ES)
Brian Sanders
AFOSR/NA
Bolling AFB DC 20332

10. SPONSORING/MONITORING AGENCY REPORT NUMBER

11. SUPPLEMENTARY NOTES

12a. DISTRIBUTION AVAILABILITY STATEMENT
Approved for public release; distribution unlimited

12b. DISTRIBUTION CODE
A

13. ABSTRACT (Maximum 200 words)

    This study investigated the residual strength of the unidirectional and cross-ply laminates of SCS-6 / Ti-15-3, metal matrix composite at elevated temperature 427°C (800°F) after under tension-tension load controlled mode. The purpose of this study was to determine the effects of different levels of fatigue damage on the composite's strength.

    The unidirectional specimens were cycled at a 900 MPa maximum stress at a frequency of 10 Hz, while, the cross-ply specimens were tested at both 300 MPa and 450 MPa at 5 Hz and 10 Hz, respectively. The residual strength results for the three cases showed similar trends in that residual strength drop with cycles was small until near the end of the fatigue life. Both the unidirectional and cross-ply specimens demonstrated only a small drop of the residual strength with cycles until near the end of the fatigue life.

14. SUBJECT TERMS
Residual Strength, Metal Matrix Composite, Life Fraction Fiber(Matrix) Dominated Failure, Fatigue, Etching, Polishing

15. NUMBER OF PAGES
92

16. PRICE CODE

17. SECURITY CLASSIFICATION OF REPORT Unclassified	18. SECURITY CLASSIFICATION OF THIS PAGE Unclassified	19. SECURITY CLASSIFICATION OF ABSTRACT Unclassified	20. LIMITATION OF ABSTRACT UL